Missouri State University

BearWorks

MSU Graduate Theses

Summer 2017

Genetic Tools to Allow Efficient Gene and Protein Characterization of the Industrially Important Bacterium Gluconobacter Oxydans

Melissa A. Schoeben
Missouri State University, Melissa833@live.missouristate.edu

As with any intellectual project, the content and views expressed in this thesis may be considered objectionable by some readers. However, this student-scholar's work has been judged to have academic value by the student's thesis committee members trained in the discipline. The content and views expressed in this thesis are those of the student-scholar and are not endorsed by Missouri State University, its Graduate College, or its employees.

Follow this and additional works at: https://bearworks.missouristate.edu/theses

 Part of the Microbiology Commons

Recommended Citation

Schoeben, Melissa A., "Genetic Tools to Allow Efficient Gene and Protein Characterization of the Industrially Important Bacterium Gluconobacter Oxydans" (2017). *MSU Graduate Theses*. 3117.
https://bearworks.missouristate.edu/theses/3117

This article or document was made available through BearWorks, the institutional repository of Missouri State University. The work contained in it may be protected by copyright and require permission of the copyright holder for reuse or redistribution.
For more information, please contact bearworks@missouristate.edu.

GENETIC TOOLS TO ALLOW EFFICIENT GENE AND PROTEIN CHARACTERIZATION OF THE INDUSTRIALLY IMPORTANT BACTERIUM *GLUCONOBACTER OXYDANS*

A Masters Thesis

Presented to

The Graduate College of

Missouri State University

In Partial Fulfillment

Of the Requirements for the Degree

Master of Science, Biology

By

Melissa A. Schoeben

May 2017

Copyright 2013 by Melissa Ann Schoeben

GENETIC TOOLS TO ALLOW EFFICIENT GENE AND PROTEIN CHARACTERIZATION OF THE INDUSTRIALLY IMPORTANT BACTERIUM GLUCONOBACTER OXYDANS

Biology

Missouri State University, May 2017

Master of Science

Melissa A. Schoeben

ABSTRACT

The acetic acid bacterium *Gluconobacter oxydans* is an industrially valuable microorganism, particularly in the production of acetic acid, D-gluconic acid, ketogluconic acids, dihydroxyacetone, and precursors for the antidiabetic drug miglitol. Despite its importance in industry, there is still much to be learned about *G. oxydans* and its many uncharacterized enzymes. Additionally, genetic engineering holds the possibility of improving current yields. However, these goals are limited, largely due to a lack of molecular tools suitable for working with the bacterium. The current molecular toolkit for *G. oxydans* specifically lacks an efficient screening system for positive clones and a system for regulatable gene expression. Therefore, two sets of fluorescent protein-based reporter systems were designed for screening and protein purification along with two sets of inducible promoter systems, the Tet and Lux systems, for the regulation of gene expression. Although, the fluorescent reporter systems were unreliable as a gene expression screening tool, the Lux inducible promoter system had reliable and strong induction of gene expression, and is a promising system to use for metabolic engineering and regulatable gene expression in *G. oxydans.*

KEYWORDS: *Gluconobacter oxydans,* fluorescent reporter, inducible promoter, fusion protein, genetic tools

This abstract is approved as to form and content

_____

Paul Schweiger, PhD
Chairperson, Advisory Committee
Missouri State University

GENETIC TOOLS TO ALLOW EFFICIENT GENE AND PROTEIN CHARACTERIZATION OF THE INDUSTRIALLY IMPORTANT BACTERIUM GLUCONOBACTER OXYDANS

By

Melissa A. Schoeben

A Masters Thesis
Submitted to the Graduate College
Of Missouri State University
In Partial Fulfillment of the Requirements
For the Degree of Master of Science, Biology

May 2017

Approved:

_____
Paul Schweiger, PhD

_____
Laszlo Kovacs, PhD

_____
Christopher Lupfer, PhD

_____
Julie Masterson, PhD: Dean, Graduate College

ACKNOWLEDGEMENTS

I would like to express my gratitude to Dr. Schweiger for allowing me to work in his laboratory and for his help and guidance with my research and thesis. I would also like to thank my committee members, Dr. Kovacs and Dr. Lupfer, for taking the time to read and critique my thesis. Thank you to the Graduate College and the Biology Department for providing funding for my research. I would like to acknowledge my labmates Marshal Blank, Kyle Ess, and Kevin martin. Thank you to Dr. Kathy Hughes, Dr. John Steiert, and Rhy Norton for their letters of recommendation. Finally, I would like to thank my husband, Mark, for his support and encouragement throughout my time as a student.

TABLE OF CONTENTS

LIST OF TABLES

LIST OF FIGURES

INTRODUCTION

Gluconobacter oxydans 621H

Gluconobacter oxydans is a gram negative, rod shaped, obligately aerobic, acetic acid bacterium. Carbon sources utilized by *Gluconobacter* include D-mannitol, D-glucose, D-fructose, sorbitol, and glycerol, and it requires pantothenic acid, niacin, thiamine, and *p*-aminobenzoic acid for growth (Gupta et al., 2001). As member of the family *Acetobacteraceae, Gluconobacter* can be distinguished from its close relative *Acetobacter* by its inability to completely oxidize acetate and lactate to CO_2 and H_2O (Gossele et al., 1983). Because of its ability to incompletely oxidize carbohydrates, alcohols, polyols, and their derivatives in a stereo- and regiospecific manner, it has become valuable in industry, especially in the production of acetic acid, the antidiabetic drug miglitol, vitamin C, D-gluconic acid, ketogluconic acids, and dihydroxyacetone (Deppenmeier et al., 2002). Many of these products are the result of reactions catalyzed by membrane-bound dehydrogenases that feed electrons into the respiratory chain (Deppenmeier et al., 2002). Among the most important are three sorbitol dehydrogenases involved in the oxidation of D-sorbitol to L-sorbose (used for vitamin C production), namely a flavoprotein sorbitol dehydrogenase, a quinoprotein sorbitol dehydrogenase, and a D-sorbitol dehydrogenase (Matsushita et al., 2003). Glucose dehydrogenase, another quinoprotein, produces gluconate (Levering et al., 1988), which is then oxidized by the flavoprotein D-gluconate dehydrogenase to 2-keto-D-gluconate (Matsushita et al., 2003) or by a polyol/glycerol dehydrogenase to 5-ketogluconate. 2-Keto-D-gluconate and 5-ketogluconate are precursors to tartaric acid. Glycerol is converted to the tanning agent

dihydroxyacetone by the polyol/glycerol dehydrogenase (Gupta et al., 2001). Lactate dehydrogenase produces pyruvate, which is used by chemical and pharmaceutical industries (Deppenmeier et al., 2002; Peters et al. 2013b). *Gluconobacter* also contains cytosolic NAD(P)/H-dependent oxidoreductases that may have important industrial applications. For example, the xylitol dehydrogenase reduces D-xylulose to the artificial non-cariogenic sweetener xylitol.

Molecular Tools for *Gluconobacter*

Despite its value in multiple industrial applications, many of its oxidoreductases remain uncharacterized as their heterologous expression and purification in the molecular biology model organism *Escherichia coli* was unsuccessful (20/75, Schweiger et al. unpublished results). Homologous expression and purification of these remaining proteins provides the possibility of characterization and expression in the native host and is not expected to be problematic. Yet, these attempts have been hindered largely due to a limited availability of bioengineering tools suitable for working with *G. oxydans*. However, recently some progress has been made due to the development of several deletion systems and expression vectors compatible with *G. oxydans* (Peters et al., 2013a; Kostner et al., 2013; Kallnik et al., 2010).

The most commonly used expression vectors for homologous and heterologous gene expression in *G. oxydans* are the pBBR1p452 and pBBR1p264 vectors that are based on the broad-host-range plasmid pBBR1MSC-2 (Kallnik et al., 2010). These vectors contain either a constitutively moderate (p452) or a strong (p264) promoter. Both contain a kanamycin resistance cassette for antibiotic selection (Figure 1). These vectors

have recently been modified to facilitate the export of proteins outside the cell and into the periplasmic space by adding a PelB signal peptide from *Erwinia carotovora* (Kosciow et al., 2014). More recently, the novel promoter *gHp0169* was identified and is recognized by *G. oxydans* (Shi et al., 2014).

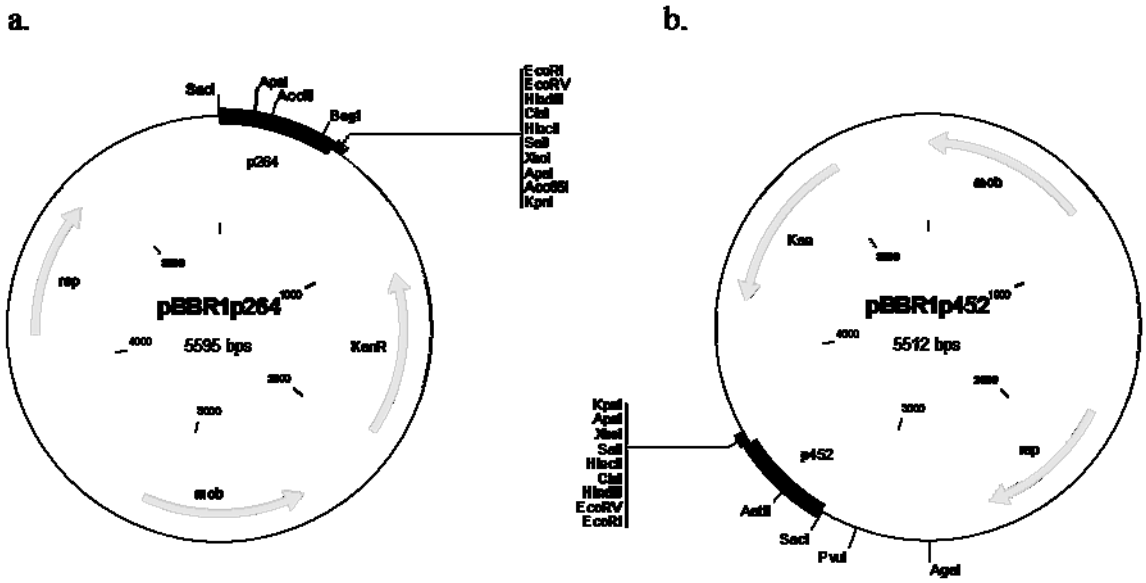

Figure 1. Original expression vectors designed for use in *G. oxydans*. (a) Plasmid pBBR1p264 with constitutive strong promoter p264; (b) Plasmid pBBR1p452 with constitutive moderate promoter p452 (Kallnik et al. 2010).

For gene deletion two systems exist, namely the *upp* and *cod* systems (Peters et al., 2013a; Kostner et al., 2013). The *upp* system relies on a special strain of *G. oxydans* 621H lacking the native *upp* gene, *G. oxydans* Δ*upp*. It is based on counter selection by reintroducing the *upp* gene, encoding a uracil phosphoribosyl transferase, to the mutant strain via a non-replicative plasmid that also encodes kanamycin resistance (Peters et al., 2013a). When transformants are grown in the presence of kanamycin the plasmid is integrated into the chromosome. Upon addition of toxic 5-fluorouracil, the plasmid loops out resulting in either wildtype or a markerless deletion. If the plasmid remains in the

chromosome, 5-fluorouracil is channeled into uracil metabolism by the plasmid encoded *upp* gene product causing fluorinated uracil incorporation into nucleic acids and eventually cell death. To eliminate the need for this special mutant strain and to enable use of wildtype bacteria the *cod* system was developed (Kostner et al., 2013). This is also a counter selection method where the nontoxic 5-fluorocytosine is converted by a non-replicative plasmid encoded cytosine deaminase, *codA*, to the toxic 5-fluorouracil that acts in the same manner as the *upp* system. More recently, the *cod* deletion system was used to create a leaky outer membrane mutant strain of *G. oxydans* to facilitate the extracellular hydrolysis of polysaccharides (Kosciow et al., 2016). This was done by deleting the *gox1687* gene encoding TolB. The resulting Δ*tolB* strain, when engineered to express an enzyme fused to the PelB signal sequence, secretes high yields of the enzyme into the medium.

Fluorescent Protein-based Reporter Systems

When attempting to characterize proteins, it can be advantageous to overproduce the protein of interest. This is done by inserting the gene that codes for the protein into an expression vector, transforming that vector into a bacterial cell, and then plating on selective medium. Because vectors that do not contain the gene of interest can be introduced along with the recombinant plasmid, it is necessary to screen for positive clones, which can be time consuming and labor intensive in *G. oxydans*. This bacterium contains 5 native plasmids (Prust et al., 2005), which makes screening by classic plasmid purification and restriction digestion unfeasible. Furthermore, rapid colony PCR techniques that are well established in *E. coli* are often unreliable in *G. oxydans*

(Schweiger et al. unpublished results). To streamline the screening process in *G. oxydans*, and to aid in protein purification, a fluorescent-based reporter system was designed. This involved the creation of vectors containing a multiple cloning site (MCS), a protease cleavage site, fluorescent reporter gene (FP), and StrepTag, all under the control of a constitutive promoter (Promoter-MCS-Protease-FP-STL) (Figure 2a). Transcripts of these base vectors lack a ribosomal binding site (RBS) and should not be translated, so fluorescence should not be produced in transformed cells. Once the gene of interest with its RBS is cloned into the MCS (Figure 2b), translation of the fusion product should cause fluorescence in positive clones. The addition of the protease cleavage site and the StrepTag to the fusion product allows for purification of tagless protein. The StrepTag will bind the fusion protein to a column containing streptavidin. The protein of interest can be released from the rest of the fusion product by adding Xa protease (Pearson, 2014) (Figure 2c).

Inducible Promoters

Another problem that needs to be overcome when overexpressing proteins is that protein overproduction can be toxic to the bacterial cell (Skerra, 1994). To mitigate reduced product yields that result from cell toxicity, it is advantageous to suppress expression of the target protein until cultures have reached a high cell density and then induce expression. Two sets of regulatable promoter/operator systems were designed to regulate gene expression in *G. oxydans*. The first was an anhydrotetracycline (ATc) inducible system in which the tetracycline repressor (TetR) is constitutively expressed and is bound to the tetracycline promotor/operator (pTet) in the absence of ATc,

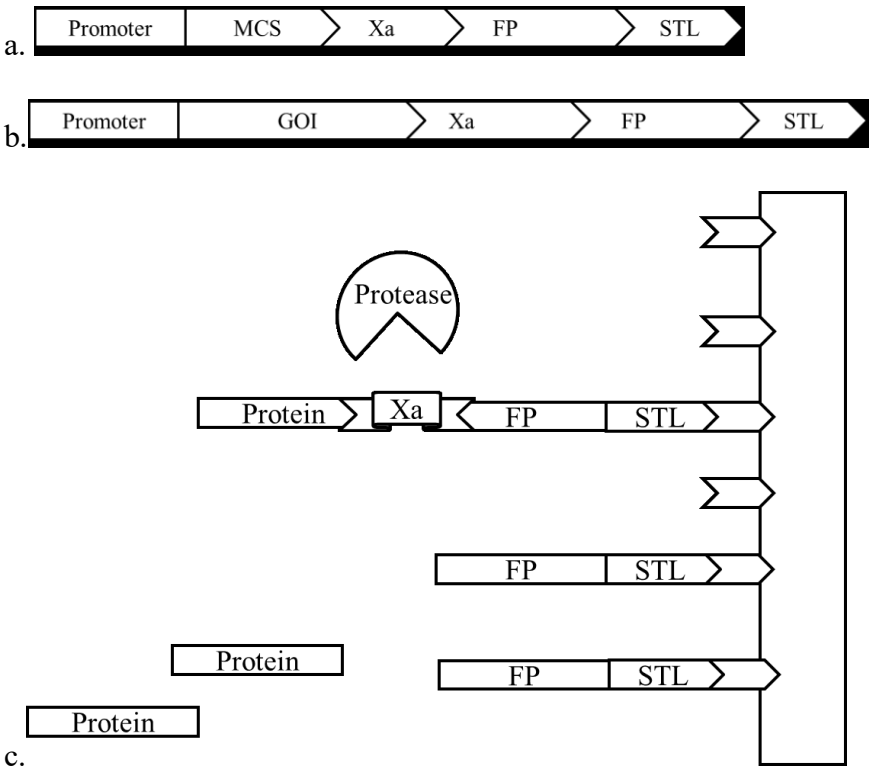

Figure 2. Fluorescent reporter fusion products and protein purification scheme. (a) Fusion product with the MCS, protease recognition site Xa, fluorescent protein (FP) and StrepTag (STL) under the control of the constitutive promoter; (b) Fusion product with the gene of interest (GOI), protease recognition site Xa, FP, and STL under the control of the constitutive promoter; (c) Protein purification scheme by affinity chromatography. The StrepTag binds the fusion protein to streptavidin. Protease is added to the column, cleaving at the Xa site, releasing the target protein.

repressing gene expression. Upon ATc addition, the repressor is released from pTet and gene expression is turned on (Figure 3). The second system was inducible by acyl-homoserine lactone (AHL), in which the Lux activator (LuxR) is constitutively expressed, but is unbound to the Lux promoter/operator (pLux) in the absence of AHL and gene expression is turned off (Figure 3). In these two systems, the native gene(s) encoding tetracycline resistance and bioluminescence, respectively (Fuqua et al., 1994; Bertrand, et al., 1983), were replaced with a multiple cloning site to allow the desired

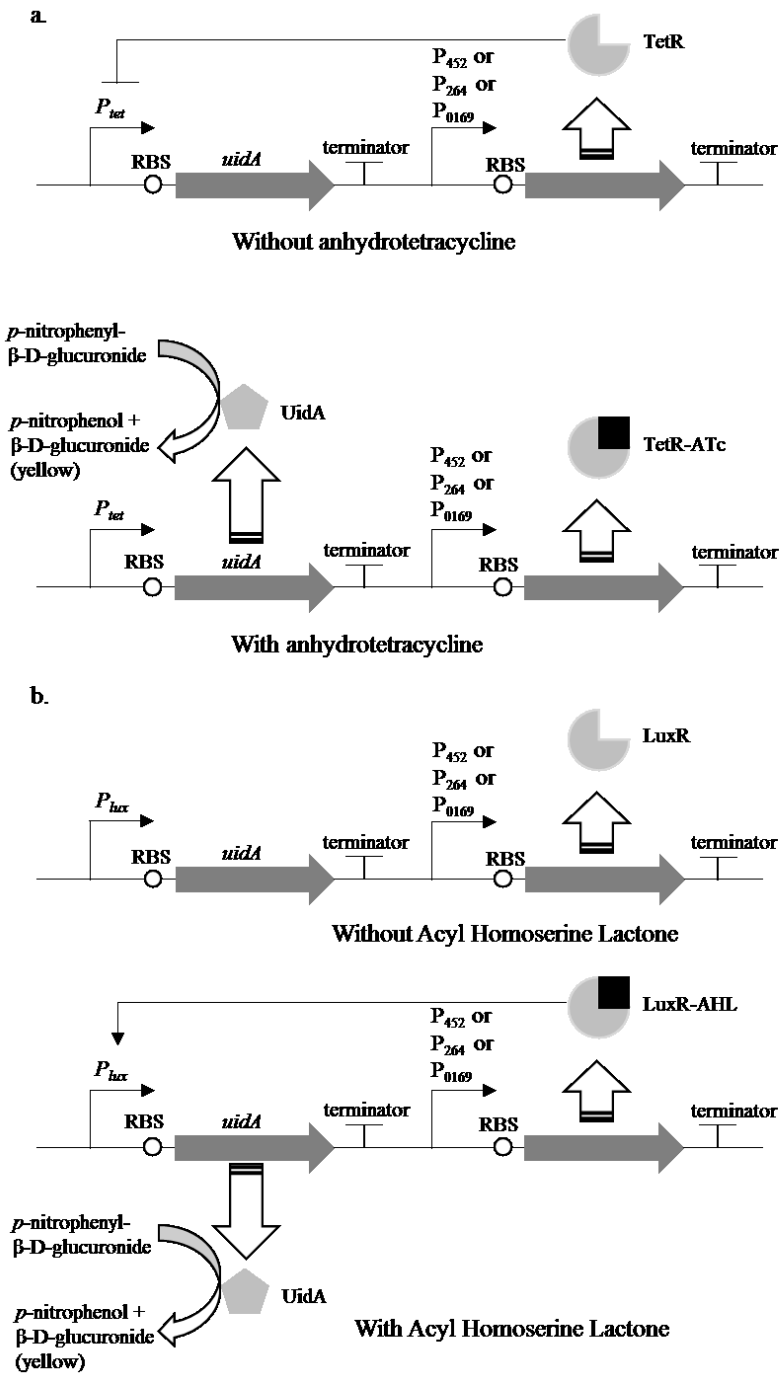

Figure 3. Scheme of proposed regulatable promoter elements. (a.) Regulation of the Tet promoter/operator system. (b.) Regulation of the Lux promoter/operator system. Blunt ended arrows represent repression or transcriptional terminators. Binding of anhydrotetracycline (ATc) to TetR or acyl homoserine lactone (AHL) to LuxR induces gene expression. In the promoter-fusion, induction produces β-glucuronidase (UidA) that hydrolyzes colorless *p*-nitrophenyl-β-D-glucuronide and produces a yellow *p*-nitrophenol at a rate proportional to the amount of enzyme present, which can be used to assess promoter strength and regulation.

gene to be cloned in and controlled by the inducible promoters. To evaluate and quantify gene expression, the *uidA* gene encoding a β-D-glucuronidase was used as it produces a measurable yellow color when it hydrolyzes 4-nitrophenyl-β-D-glucuronide (PNPG) (Miller, 1972) (Figure 3).

MATERIALS AND METHODS

Bacteria, Growth Conditions, and Storage

Gluconobacter oxydans 621H (DSMZ 2343), *Escherichia coli* 10β (New England Biolabs), and *Aliivibrio fischeri* (ATCC 7744) were used in these studies. *G. oxydans* 621H was grown in yeast mannitol (YM; 6 g/L yeast extract, 20 g/L mannitol) broth with 50μg/mL cefoxitin at 30˚C and 200rpm. *E. coli* 10β was grown in lysogeny broth (LB; 5g/L yeast extract, 10g/L tryptone, 10g/L sodium chloride) with 100μg/mL streptomycin at 30-37˚C and 200rpm. *A. fischeri* was grown on marine broth (BD Difco 2216) at 30˚C and 200rpm. Agar was added to 1.5% when making solid medium. Kanamycin was added to 50μg/mL for plasmid maintenance when appropriate. For long-term storage, bacteria were kept at -80˚C in frozen stocks made from well-grown cultures with glycerol added to 15%.

Molecular Biological Techniques

Genomic DNA was extracted using a GenElute Bacterial Genomic DNA Kit (Sigma Aldrich) according to the manufacturer's instructions. Plasmids were purified using a GeneJET Plasmid Miniprep Kit (ThermoFisher Scientific) according to manufacturer's instructions. DNA was purified from agarose gels and PCR reactions prior to ligations using the GeneJet Gel Extraction and DNA Cleanup Micro Kit (ThermoFisher Scientific) or the Wizard SV Gel and PCR Cleanup Kit (Promega) using the recommended protocols.

Electrophoresis was performed using a 0.7% agarose gel to determine the approximate size of DNA fragments or to separate them for purification. Ethidium bromide was added directly to the gel at a final concentration of 0.5 µg/mL for visualization of nucleic acids. Agarose gels were prepared with 1x TAE buffer (40 mM Tris base, 1 mM EDTA, 20 mM glacial acetic acid, pH 8.6) and run at 100 – 120 V. DNA samples were mixed with 6x loading dye (ThermoFisher Scientific) prior to loading the gel. A Gene Ruler 1Kb DNA Ladder (ThermoFisher Scientific) was used as a marker. Gels were viewed and photographed over a UV light using a FOTO/Analyst Apprentice System (Fotodyne Inc, Hartland, WI).

DNA was digested using FastDigest or ThermoFisher Scientific restriction endonucleases (ThermoFisher Scientific) in 20-30µL reactions according to manufacturer's recommendations. Digested PCR fragments were ligated into similarly cut and purified vectors in a 20µL reaction volume at a 3:1 mol ratio using T4 DNA Ligase (ThermoFisher Scientific). Reactions were incubated at 16˚C for 16-24 hours. When possible 1.0-0.5 µl of a restriction enzyme that cuts the vector, but not the desired construct was added post-ligation to reduce self-ligated vector and uncut vector background.

Sanger sequencing was used to confirm all constructs and was performed by Eurofins Genomics using primers pBBR1_for, pASK_rev, MCSseq_F, or MCSseq_R. Synthetic genes were codon optimized for *G. oxydans* 621H and synthesized by GenScript (Piscataway, NJ) or Eurofins Genomics.

Gradient PCR was performed to determine the optimal annealing temperature for PCR primers (Table 1). DreamTaq DNA Master Mix (ThermoFisher Scientific) was used

according to the manufacturer's recommended instructions using the following amplification cycling: 95˚C for 5 min, followed by 30-35 cycles of 95˚C 10 s, 50-70˚C 30 s, 72˚C 1 min/kb and a final extension of 72˚C for 5 min. The high fidelity Phusion DNA Polymerase (ThermoFisher Scientific) was used to amplify cloning targets according the recommended conditions using the following amplification cycling: 98˚C for 2 min, followed by 30-35 cycles of 98˚C 10 s, annealing temperature 30 s, 72˚C 15 s/kb for plasmid templates or 30 s/kb for genomic DNA templates and a final extension of 72˚C for 5 min. When not determined by gradient PCR, annealing temperature was determined using the New England Biolabs Tm Calculator (http://tmcalculator.neb.com/#!/).

Colony PCR was done to screen for positive transformants. *E. coli* colonies were picked from plates using sterile wooden toothpicks, mixed with 50µL of sterile nuclease-free water, and 5µL was used as a template for colony PCR. To the remaining cell suspension, 150µL of LB was added and used as an inoculum for 5 mL cultures of positive transformants. *G. oxydans* transformants were streaked onto a quadrant of YM agar and incubated until growth occurred. Cells were then picked as described for *E. coli.* Dream Taq DNA Master Mix Polymerase (ThermoFisher Scientific) was used to amplify the target sequence according to the manufacturer's recommended instructions using the following amplification cycling: 95˚C for 5 min, followed by 30-35 cycles of 95˚C 10 s, annealing temperature 30 s, 72˚C 1 min/kb and a final extension of 72˚C for 5 min.

Construction of Fluorescent Reporter Systems

Two fluorescent protein reporter systems were created using pBBR1p264-pelB-STL and pBBR1p452-STL as backbones. The genes encoding the fluorescent proteins

Table 1: Primers

Primer	Sequence	RE
Xa-GFPuvRBS_F	ATGCTACGTAATCGATGGTCGCATGAGTAAAGG AGAAGAAC	SnaBI
GFPuv_R	ATCGGCGCGCCTTTGTAGAGCTCATCCATGCCAT	AscI
Gox0265_EcoRI_F	ATGGAATTCTGACATCTTGACCCTTGACG	EcoRI
Gox0265_SnaBI_R	ATGTACGTATTTCtGATCGGGCAGGGC	SnaBI
Gox2015_EcoRI_R	ATGGAATTCTCAAACCTGCATTCACAAGG	EcoRI
Gox2015_SnaBI_R	ATGTACGTACGAGGACCAGTTGTTTTCG	SnaBI
RFPf	ATGCTACGTAATCGATGGTCGCATGGCCTCCTCC GAGGACGTC	SnaBI
RFPr	CGGTGGCGCGCCGGCGCCGGTGGAGTGGCGGC	AscI
rbsRFPf	TGCAGGAATTCAGGAGGTAATATTTATGGCCTCC TCCGAGGACGTC	EcoRI
p0169_F	ATGCAGAGCTCTGAAAGCGGCTGGCGCGT	SacI
p0169_R	ATGCAGAATTCGCGGAAGGCGTTATACCCTGA	EcoRI
EcoRI/RBS/tetR_F	ATGAGAATTCAAAGAGGAGAAATACTAGATGT CTCGTTTAGATAAAAG	EcoRI
BsaI_uidA_F	ATGGTAGGTCTCAAATGTTACGTCCTGTAGAAAC CCCAAC	BsaI
BsaI_uidA_R	ATGGTAGGTCTCATATCATTGTTTGCCTCCCTGC TGCGG	BsaI
EcoRI/RBS/luxR_F	ATGAGAATTCAAAGAGGAGAAATACTAGATGAA AAACATAAATGCCGAC	EcoRI
luxR_R	ATGAGGTCTCAAGCTGTTAATTTTTAAAGTATG GGC	BsaI

RE, Restriction endonucleases are underlined.
* Indicates primers used for sequencing.

Table 1: Primers continued

Primer	Sequence	RE
MluI/RBS/luxR_F	ATGAACGCGTAAAGAGGAGAAATACTAGATGA AAAACATAAATGCCGAC	MluI
TetR_R	ATGAAAGCTTTTAAGACCCACTTTCACAT	HindIII
MluI/RBS/tetR_F	ATGAACGCGTAAAGAGGAGAAATACTAGATGT CTCGTTTAGATAAAAG	MluI
pTet_F	GCTCGAATGCCCCAGGGTC	PasI
pTet_R	CGAGCGCATTGTATACGAG	Bst1107I
MCSseq_F*	CTGTTCCGTCAGCAGCTTTT	-
MCSseq_R*	GTAGGCGGTCACGACTTTG	-
pBBR1-for*	ACTCACTATAGGGCGAATTG	-
pASK_rev*	CGCAGTAGCGGTAAACG	-

RE, Restriction endonucleases are underlined.
* Indicates primers used for sequencing.

GFPuv and mRFP were amplified with Phusion DNA polymerase using Xa-GFPuvRBS_F and GFPuv_R for GFPuv or RFPf and RFPr for mRFP. Primers contained 5' restriction sites for SnaBI (forward) and AscI (reverse). The forward primer also contained the sequence for the Xa protease cleavage site to create the amplicons Xa-GFPuv or Xa-mRFP. The amplicons were then digested with SnaBI and AscI and ligated into the similarly cut pBBR1p264-pelB-STL and pBBR1p452-STL vectors to create pBBR1p(264/452)-Xa-(GFPuv/mRFP)-STL and transformed into E. coli 10β for plasmid maintenance. Vectors were isolated from E. coli 10β and transformed into electrocompetent G. oxydans 621H.

Two *G. oxydans* genes, *gox0265* and *gox2015* (Prust et al., 2005), were cloned into the multiple cloning site (MCS) of pBBR1p(264/452)-Xa-(GFPuv/RFP)-STL to act as proof of concept for the fluorescent reporter systems. The genes were amplified with Phusion DNA polymerase using primers containing 5' restriction sites EcoRI (forward primer) and SnaBI (reverse primer). The amplified fragments were cut with EcoRI and SnaBI and then ligated into similarly cut pBBR1p(264/452)-Xa-(GFPuv/mRFP)-STL vectors. These vectors were transformed into *E. coli* 10β for plasmid maintenance. Vectors were isolated from *E. coli* 10β and transformed into electrocompetent *G. oxydans* 621H cells.

Construction of Inducible Promoter Systems

TetR System. The *tetR* gene was amplified from a pASK-IBA3 plasmid (IBA GmbH, www.iba-lifesciences.com) using MluI/RBS/tetR_F or EcoRI/RBS/tetR_F and TetR_R primers containing 5' restriction sites MluI (forward primer) or EcoRI (forward primer) and HindIII (reverse primer) (Table 1). The amplified fragments were purified as described above, were cut with EcoRI and HindIII, and ligated into similarly cut pBBR1p452-STL to create p452TetR. Alternatively, purified PCR products were cut with MluI and HindIII and ligated into similarly cut pBBR1p264-pelB-STL to create p264TetR. To create p0169TetR, *p0169* was amplified from *G. oxydans* DNA with primers containing the 5' restriction sites SacI and EcoRI. The amplified fragments were purified and cut with SacI and EcoRI and then ligated into similarly cut p452TetR. These vectors were transformed into *E. coli* 10β for plasmid maintenance. Positive

transformants were screened by colony PCR and isolated plasmids were screened by restriction digest and confirmed by sequencing

The tetracycline promotor and MCS fragment was designed with a Tet promotor (iGEM part BBa_R0040) upstream of a ribosomal binding site (iGEM part BBa_B0034) and a MCS region containing 2 BsaI restriction sites derived from pASK-IBA3 (IBA GmbH, www.iba-lifesciences.com). A transcriptional terminator (iGEM part BBa_B0010) was added downstream of the MCS. The fragment was synthesized and cloned into a pUC57 plasmid by GenScript (Table 2). The pTet-MCS region was amplified using pTet_F and pTet_R primers with the 5' restriction sites PasI (forward primer) and Bst1107I (reverse primer) then purified. The amplified fragments were cut with PasI and Bst1107I and ligated into similarly cut p0169TetR, p264TetR, and p452TetR plasmids to create p(0169/264/452)pTet (Table 2). These vectors were transformed into *E. coli* 10β for plasmid maintenance. Positive transformants were screened by colony PCR and isolated plasmids were screened by restriction digest, sequenced and transformed into *G. oxydans*. Positive *G. oxydans* were confirmed by colony PCR and sequencing.

The *uidA* gene was amplified using BsaI_uidA_F and BsaI_uidA_R primers with BsaI restriction sites and purified. The amplified fragments were cut with BsaI and ligated into similarly cut and purified p(0169/p264/p452)pTet plasmids creating p(0169/p264/p452)pTet-uidA to act as proof of concept for the inducible Tet system. These vectors were transformed into *E. coli* 10β for plasmid maintenance. Positive transformants were screened by colony PCR and sequencing prior to transforming into *G. oxydans*. Positive *G. oxydans* were confirmed through colony PCR.

Table 2: Plasmids used in this study

	Plasmid	Description
P1	pBBR1p264-pelB-STL	pBBR1MCS-2 derivative with strong promoter p264, KanR, MCS, pelB signal sequence and StepTag (Kallnik et al., 2010; Kosciow et al., 2014).
P2	pBBR1p452-STL	pBBR1MCS-2 derivative with moderate promoter p452, KanR, MCS, and StepTag (Kallnik et al., 2010).
P3	pBBR1p264-Xa-GFPuv-STL	P1 derivative with Xa-GFPuv
P4	pBBR1p452-Xa-GFPuv-STL	P2 derivative with Xa-GFPuv
P5	pBBR1p264-*gox2015*-Xa-GFPuv-STL	P3 derivative with *gox2015*
P6	pBBR1p452-*gox2015*-Xa-GFPuv-STL	P4 derivative with *gox2015*
P7	pBBR1p264-*gox0265*-Xa-GFPuv-STL	P3 derivative with *gox0265*
P8	pBBR1p452-*gox0265*-Xa-GFPuv-STL	P4 derivative with *gox0265*
P9	pBBR1p264-Xa-mRFP-STL	P1 derivative with Xa-mRFP
P10	pBBR1p452-Xa-mRFP-STL	P2 derivative with Xa-mRFP
P11	pBBR1p264-*gox2015*-Xa-mRFP-STL	P9 derivative with *gox2015*
P12	pBBR1p452-*gox2015*-Xa-mRFP-STL	P10 derivative with *gox2015*
P13	pBBR1p264-*gox0265*-Xa-mRFP-STL	P9 derivative with *gox0265*
P14	pBBR1p452-*gox0265*-Xa-mRFP-STL	P10 derivative with *gox0265*
P15	p264LuxR	P1 derivative with LuxR
P16	p452LuxR	P2 derivative with LuxR
P17	p0169LuxR	P16 derivative with p0169
P18	p264pLux	P15derivative with pLux
P19	p452pLux	P16 derivative with pLux
P20	p0169pLux	P17 derivative with pLux
P21	p264pLux-uidA	P18 derivative with uidA

Table 2: Plasmids used in this study continued

	Plasmid	Description
P22	p452pLux-uidA	P19 derivative with uidA
P23	p0169pLux-uidA	P20 derivative with uidA
P24	p264TetR	P1 derivative with TetR
P25	p452TetR	P2 derivative with TetR
P26	p0169TetR	P25 derivative with p0169
P27	p264pTet	P24 derivative with pTet
P28	p452pTet	P25 derivative with pTet
P29	p0169pTet	P26 derivative with pTet
P30	p264pTet-uidA	P27 derivative with uidA
P31	p452pTet-uidA	p28 derivative with uidA
P32	p0169pTet-uidA	p29 derivative with uidA
P33	pUC-57-pTet	Cloning vector with MCS, LacZ promoter, AmpR, pTet
P34	pASK-IBA3	Expression plasmid with StrepTag, Tet promoter/operator, AmpR (IBA GmbH)

LuxR System. The *luxR* gene was amplified with Phusion DNA polymerase from *A. fischerii* DNA using MluI/RBS/luxR_F or EcoRI/RBS/luxR_F and LuxR_R primers containing MluI, EcoRI, and BsaI 5' restriction sites, respectively (Table 1). The amplified fragments were cut with either MluI or EcoRI and BsaI for ligation into pBBR1p452-STL (cut with EcoRI and HindIII) or pBBR1p264-pelB-STL (cut with MluI and HindIII) to create p452LuxR and p264LuxR, respectively. To create p0169LuxR, *p0169* was amplified from *G. oxydans* with p0169_F and p0169_R primers containing

the 5' restriction sites SacI and EcoRI. The amplified fragments were purified and cut with SacI and EcoRI and then ligated into similarly cut p452LuxR. These vectors were transformed into *E. coli* 10β for plasmid maintenance. Positive transformants were screened by colony PCR and isolated plasmids were screened by restriction digest prior to sequence confirmation.

The Lux promotor and MCS fragment (pLuxMCS) was designed with a Lux promotor upstream of a ribosomal binding site (iGEM parts BBa_R0062 and BBa_B0034) and a MCS region containing two BsaI restriction sites derived from pASK-IBA3. The iGEM BBa_B0010 transcriptional terminator was again added downstream of the MCS. The pLuxMCS fragment was synthesized by Eurofins Genomics. The synthesized fragment was cut with PasI and Bst1107I and ligated into similarly cut p0169LuxR, p264LuxR, and p452LuxR plasmids to create p(0169/264/452)pLux. These vectors were transformed into *E. coli* 10β for plasmid maintenance. Positive transformants were screened by colony PCR and isolated plasmids were screened by restriction digest, sequenced and transformed into *G. oxydans*. Positive *G. oxydans* were confirmed through colony PCR. To monitor gene expression in this system, the *uidA* gene was amplified and cloned in the same way as described for the TetR system except the *uidA* gene was inserted into the p(0169/p264/p452)pLux plasmids creating p(0169/p264/p452)pLux-uidA.

Preparation of Competent Cells and Transformation

Chemically competent *E. coli* 10β cells were prepared according to the modified method of Chung et al., 1989. Briefly, *E. coli* 10β cultures were grown to an OD_{600} of

0.3-0.6. The cells were then centrifuged at 4˚C and 3000rpm for 10 minutes. After centrifugation, the cells were resuspended in 100µL ice cold sterile TSS (10% polyethylene glycol 8000, 5% dimethyl sulfoxide, 50 mM $MgCl_2$, pH 6.5). The cells suspensions were incubated with 100ng DNA on ice for 30 minutes and heat shocked at 42˚C for 90 seconds, 900 µL LB was added and the cells were incubated at 30˚C and 200rpm for 1 hour. The cells were then plated on LB agar with 50µg/mL kanamycin and incubated overnight at 37˚C.

Electrocompetent *G. oxydans* cells were prepared using a modified method of Kallnik et al. (2010). *G. oxydans* 621H cultures were grown to an OD600 of 0.6-1.0. The cells were transferred to centrifuge tubes and incubated on ice for 30 minutes and then centrifuged at 4˚C and 4000rpm for 10 minutes. Cells were then washed 3 times in the original volume of cold, sterile 1mM HEPES solution by resuspending and centrifuging cells at 4˚C and 4000rpm for 10 minutes. Cells were resuspended in 250µL 1mM HEPES and 20µL of sterile 75% glycerol was added per 100µL of cell suspension. Cells were divided into 50µL aliquots, flash frozen in liquid nitrogen, and then stored at -80˚C or used immediately for transformation. For transformation, frozen 50µL aliquots of *G. oxydans* 621H cells were thawed on ice and then mixed with 1-2µL of plasmid. The cells were transferred to a sterile 0.1 cm electroporation cuvette and pulsed at 2.0 kV in a Bio-Rad MicroPulser. Immediately after electroporation 800µL of YM was mixed with the cells and transferred to a sterile 15mL conical tube. The cells were incubated at 30˚C and 200rpm overnight and plated on YM with 50µg/mL cefoxitin and 50µg/mL kanamycin until colonies appeared.

Microscopy, β-D-Glucuronidase Assays, and Data Analysis

Fluorescent microscopy was done for GFPuv detection using an Olympus 1X81 confocal microscope with a Yokagawa CSUX1 spinning disk head and 488nm filter. Images were captured using an Image EM camera and software. For mRFP, detection an Olympus BX41 with a green filter and Olympus DP70-SBW software was used. Brightfield microscopy was done to visualize cell morphology after staining with crystal violet. Prior to microscopy, 1mL of cells were centrifuged at 13,200 rpm for 2 minutes and washed 3 times in 10X phosphate buffered saline (PBS; ChemCruz:Catalog #sc-24946), then resuspended in 100µL PBS.

Gene induction was monitored by measurement of β-D-glucuronidase (UidA) activity (in Miller Units) essentially as described (Miller, 1972). *G. oxydans* cells were grown in YM with 50µg/mL cefoxitin and kanamycin to an OD_{600} of 0.4-0.8. Cells containing the pTet system were induced with anhydrotetracycline (ATc) to final concentrations of 0, 100, 200, and 500ng/mL for 16-24 hours. Cells with the pLux system were induced with N-(3-Oxohexanoyl)-L-homoserine lactone (AHL; Chemodex) at final concentration of 0, 1, 5, and 10µM for 1 hour. After induction, 750µL aliquots of cells were centrifuged at 13,200rpm for 5 minutes. The cells were resuspended in 750µL of 50mM Tris-HCl pH 8. Cells were permeabilized by adding 30µL chloroform and 20µL 0.1% SDS, vortexed for 5 seconds, and incubating at 30˚C for 2 minutes. To a 96 well plate, 20µL of the permeabilized cells were mixed with 180µL PNPG (1mg/ml PNPG in 50mM Tris-HCl, pH 8). The plate was placed in a BioTek EL808 plate reader at 30°C, incubated for 1-4 h with shaking, and monitored at 405nm with readings taken at time

zero and every 5 min thereafter. Data were analyzed using BioTek Gen5 software. All tests were done in at least 3 biological replicates each with four replicates.

Statistical analyses and box-and-whisker plots were performed using R Studio (R Core Team, 2013; http://www.R-project.org/). Data was analyzed by performing a one-way analysis of variance (ANOVA) and a *post-hoc* Tukey's HSD test ($q = 0.05$). The R packages used in this study were dplyr, ggplot2, plyr, multcomp, and reshape2.

RESULTS

Fluorescent Protein-Based Reporter Systems

When using expression vectors to overproduce a protein in a cell, vectors that do not contain the target gene can be introduced as well as the recombinant plasmid, making it necessary to screen for positive clones. *G. oxydans* contains 5 native plasmids (Prust et al., 2005), which makes screening by classic plasmid purification and restriction digestion unfeasible. Furthermore, rapid colony PCR techniques are often unreliable in *G. oxydans*. To this end two fluorescent protein based reporter systems using either GFPuv or mRFP were created to facilitate rapid screening of positive *G. oxydans* clones and subsequent protein purification. Both reporter systems were created using the expression vectors, pBBR1p264-pelB-STL and pBBR1p452-STL as backbones. The backbone vectors contained a strong (p264) and moderate (p452) (Kallnik et al. 2010) constitutive promoter upstream of a multiple cloning site and a StrepTag sequence. The fluorescent reporter genes were amplified with forward primers designed to fuse a Xa protease recognition site upstream of the GFPuv or mRFP reporter proteins. The amplicon was then cloned into pBBR1p452-ST and pBBR1p264-pelB-STproducing the vectors pBBR1p452-Xa-(GFPuv/mRFP)-ST and pBBR1p264-Xa-(GFPuv/mRFP)-ST. Because there is no ribosomal binding site upstream of the Xa cleavage site or the fluorescent reporter, no fluorescence was expected when *G. oxydans* contained these constructs.

As a proof of concept, a cytosolic and membrane-bound glucose dehydrogenase (*gox2015* and *gox0265*) (Prust et al., 2005) containing their native ribosomal binding sites were amplified by PCR and cloned upstream and in-frame to the Xa protease site of these

vectors using restriction enzymes SnaBI and EcoRI to create translational fusions of the genes of interest, Xa site, GFP or mRFP, and StrepTag. This resulted in the construction of pBBR1p(264/452)-*gox2015*-Xa-GFPuv-STL and pBBR1(p452/264)-*gox2015*-Xa-mRFP-STL (Figures 4 and 5). Attempts to create constructs containing the *gox0265* target gene were unsuccessful. However, colony PCR screening confirmed that pBBR1p(452/264)-Xa-(GFPuv/mRFP)-STL and pBBR1p(264/452)-*gox2015*-Xa-(GFPuv/mRFP)-STL were successfully constructed (Figures 4 and 5). They were transformed into *G. oxydans* and analyzed for their ability to fluoresce. Attempts to transform *G. oxydans* with constructs containing the strong p264 promoter in combination with GFPuv were also unsuccessful.

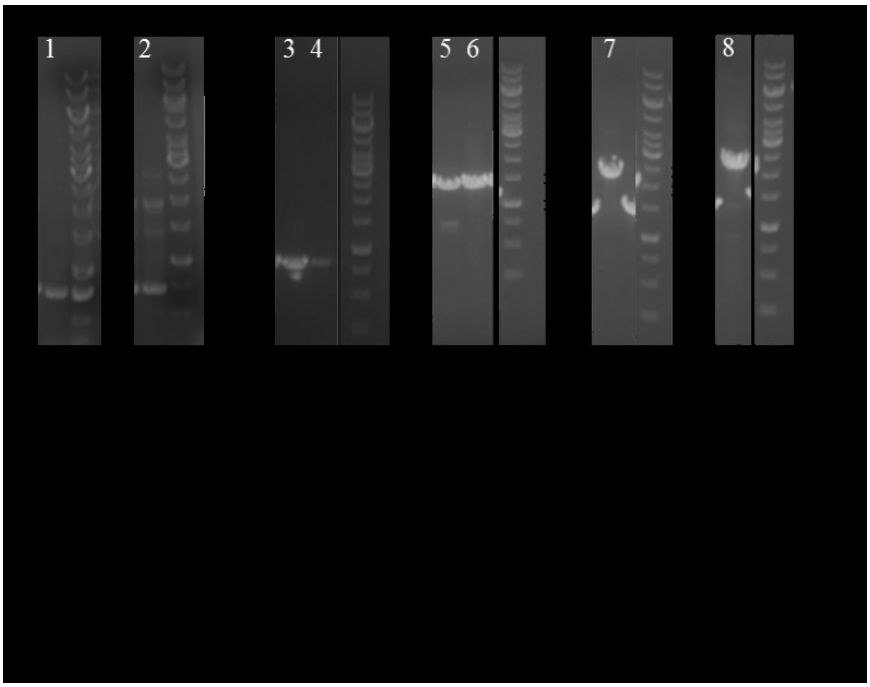

Figure 4. Agarose gels confirming positive GFPuv and mRFP constructs. (a) GFP constructs, lane 1and 2 positive colony PCR band at ~750bp, lane 3 and 4 positive colony PCR bands at ~800bp; (b) RFP constructs, lane 5 and 6 positive colony PCR bands at ~1200bp, lane 7 and 8 positive colony PCR bands at ~2300bp. The figure is a composite of multiple agarose gels adjusted to the observed sizes.

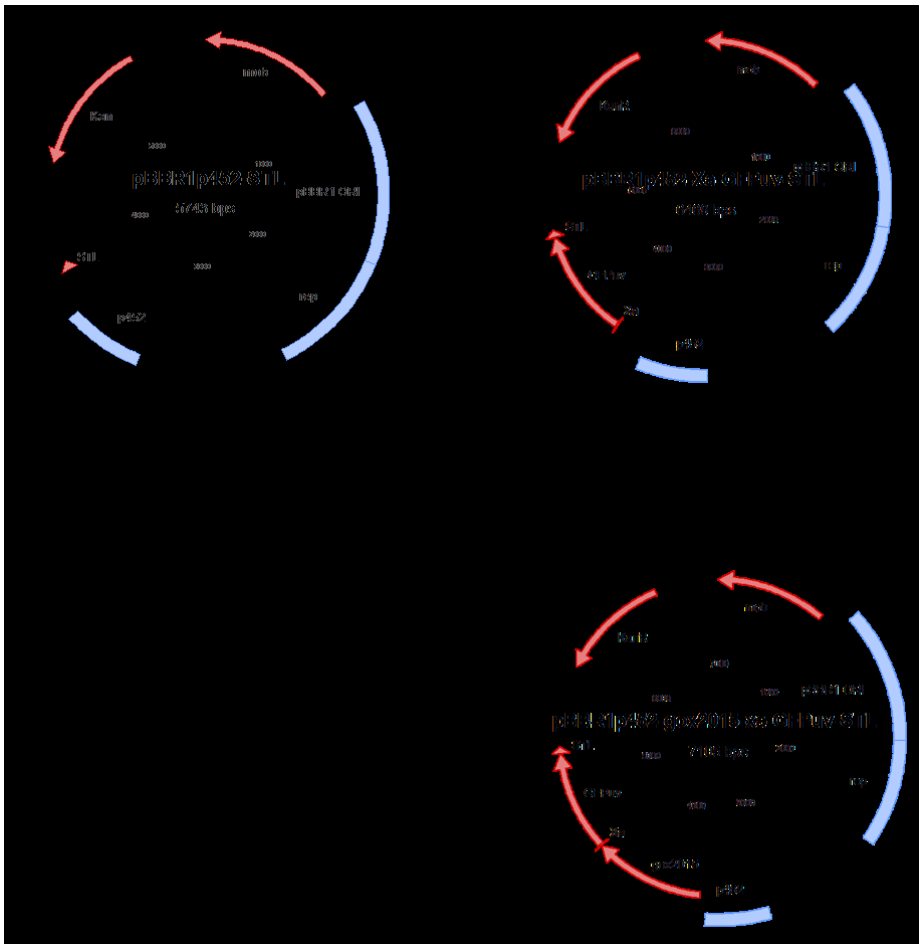

Figure 5. Construction of fluorescent-based reporter systems. Vector maps of pBBR1p452-STL, pBBR1p452-Xa-GFPuv-STL, and pBBR1p452-*gox2015*-Xa-GFPuv-STL. Vector pBBR1p452-Xa-GFPuv-STL was created by ligating Xa-GFPuv amplicon cut with AscI and SnaBI into similarly cut pBBR1p452-STL. Vector pBBR1p452-*gox2015*-Xa-GFPuv-STL was created by ligating the *gox2015* amplicon cut with SnaBI and EcoRI into similarly cut pBBR1p452-Xa-GFPuv-STL. Construction of the mRFP plasmids were done in a similar manner.

G. oxydans wildtype and those containing the pBBR1p(264/452)-Xa-(GFPuv/mRFP)-STL, pBBR1p(264/452)-*gox2015*-Xa-mRFP-STL, and pBBR1p452-*gox2015*-Xa-GFPuv-STL plasmids were grown overnight, washed three times with PBS, and visualized by fluorescent microscopy. Cells containing the pBBR1p452-*gox2015*-Xa-

GFPuv-STL had unreliable fluorescence as many cells did not fluoresce (Figure 6). Unexpectedly, cells containing empty vectors, containing only the Xa-GFPuv element also fluoresced (Figure 6). Cells containing the mRFP-based reporter systems fluoresced, including empty vectors not containing a RBS and *G. oxydans* gene to direct expression (Figure 7). However, wildtype cells did not fluoresce. One distinct difference in proof of concept constructs containing *gox2015* is that plasmids containing these genes (i.e. pBBR1p264-*gox2015*-Xa-RBS-mRFP-STL or pBBR1p452-*gox2015*-Xa-GFPuv-STL) were frequently elongated and irregularly shaped compared to those containing the pBBR1p(264/452)-Xa-mRFP-STL and pBBR1p452-Xa-GFPuv plasmids, which had wildtype *G. oxydans* morphology (Figure 6 and 7).

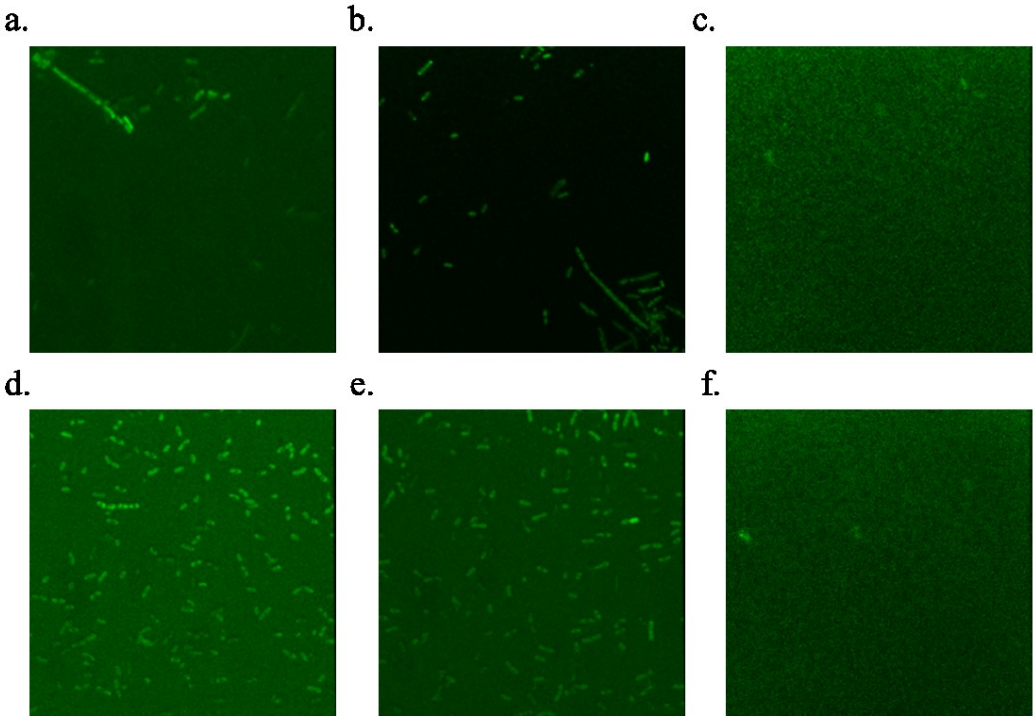

Figure 6. Fluorescent microscopy of *G. oxydans* expressing GFPuv**.** (a and b) *G. oxydans* 621H cells harboring the pBBR1p452-*gox2015*-Xa-GFPuv-STL plasmids; (c) wildtype *G. oxydans* 621H; (d and e) *G. oxydans* 621H cells harboring the pBBR1p452-Xa-GFPuv-STL plasmids; (f) wildtype *G. oxydans* 621H.

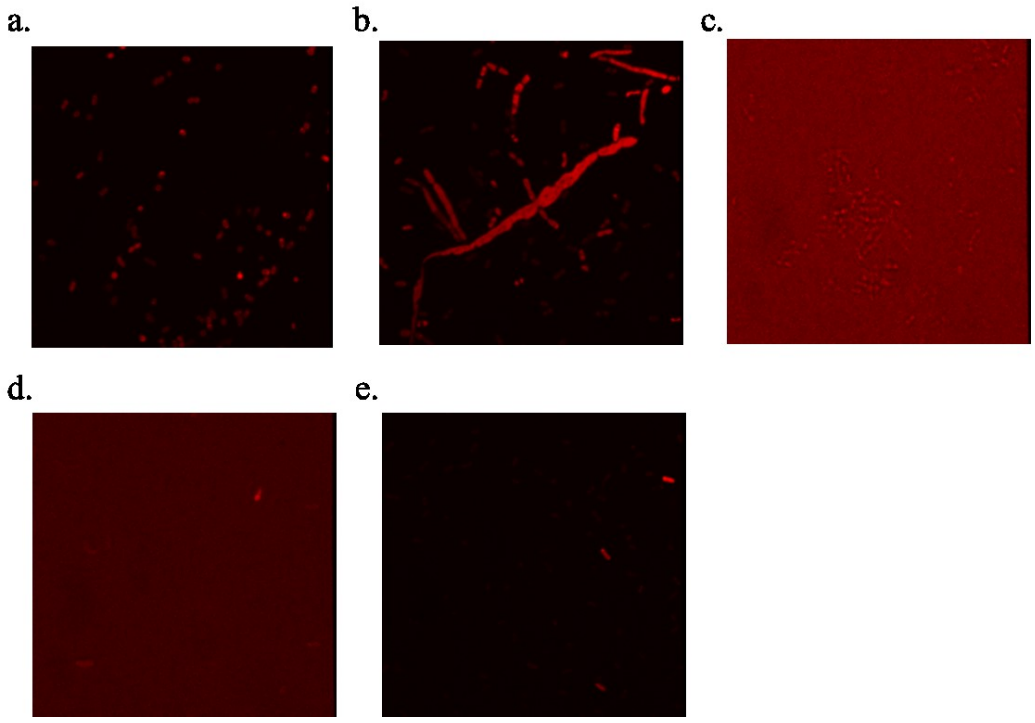

Figure 7. Fluorescent microscopy of *G. oxydans* expressing mRFP. (a) *G. oxydans* 621H cells harboring the pBBR1p264-Xa-mRFP-STL plasmids; (b) *G. oxydans* 621H cells harboring the pBBR1p264*gox2015*-Xa-mRFP-STL plasmids; (c) Wildtype *G. oxydans* 621H; (d) *G. oxydans* 621H cells harboring the pBBR1p452-Xa-mRFP-STL plasmids; (e) *G. oxydans* 621H cells harboring the pBBR1p452-*gox2015*-Xa-mRFP-STL plasmids.

Inducible Promoter Systems

Construction of AHL Inducible Promoter Systems. Three AHL inducible systems were created by cloning the *luxR* gene into pBBR1p264-pelB-STL and pBBR1p452-STL to create p264LuxR and p452LuxR (Figure 8 and 9). The promoter p452 was then replaced with p0169 (Shi et al., 2014) in the p452LuxR plasmid to create p0169LuxR (Figure 9). A synthesized DNA fragment containing the Lux promoter, RBS, MCS, and terminator (Florea et al., 2016) (Figure 9e) was cloned into the p264LuxR, p452LuxR, and p0169LuxR plasmids to create p264pLux, p452pLux, and p0169pLux (Figure 8 and 9). Proof of concept constructs were created by cloning *uidA* into the MCS of p264pLux, p452pLux, and p0169pLux to create p264pLux-uidA, p452pLux-uidA, and

p0169pLux-uidA (Figure 8 and 9). The p264pLux, p452pLux, p0169pLux, p264pLux-uidA, p452pLux-uidA, and p0169pLux-uidA were all transformed by electroporation into *G. oxydans*.

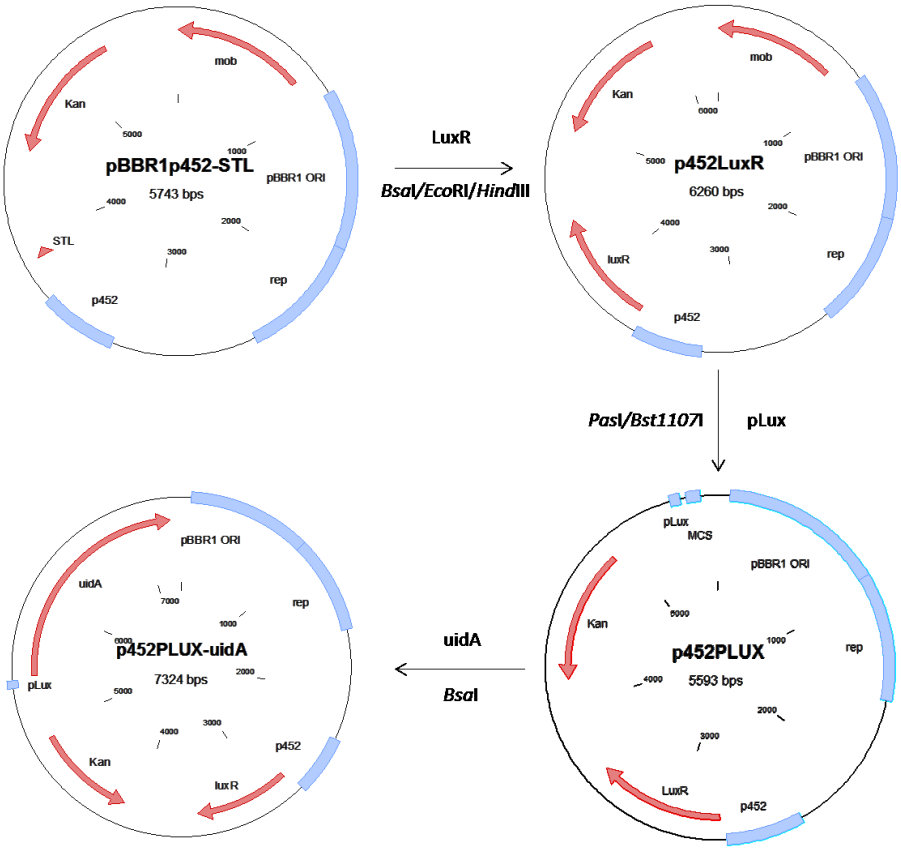

Figure 8. Construction of the Lux system. Vector maps of pBBR1p452-STL, p452LuxR, p452pLux, and p452pLux-uidA. Plasmid p452LuxR was created by ligating LuxR amplicon cut with BsaI and EcoRI into a pBBR1p452 plasmid cut with EcoRI and HindIII. Plasmid p452pLux was created by ligating the pLux DNA fragment cut with PasI and Bst1107I with similarly cut p452LuxR. Plasmid p452pLux-uidA was created by ligating the *uidA* amplicon cut with BsaI into similarly cut p452pLux. Construction of p264pLux-uidA and p0169pLux-uidA were done similarly.

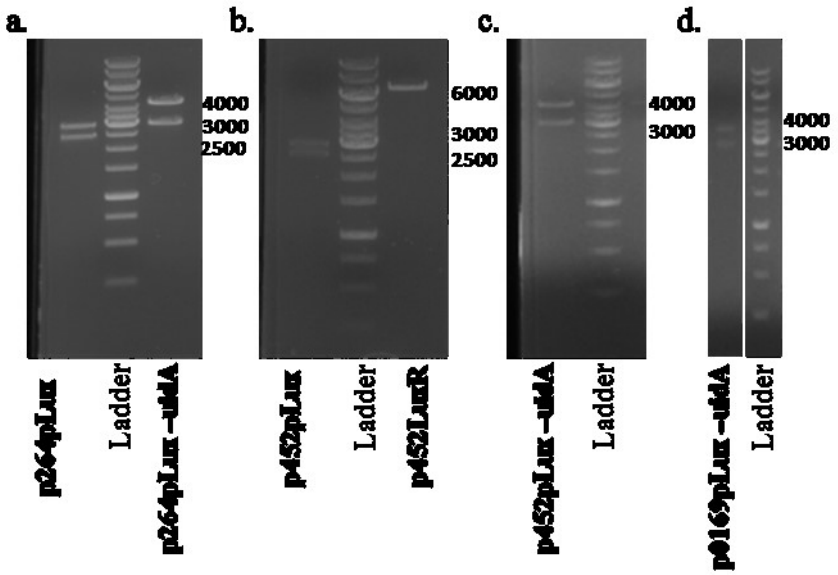

e.

ACCTGTAGGATCGTACAGGTTTACGCAAGAAAATGGTTTGTTATAGTCGAAT
AAATACTAGTGAAAGAGGAGAAATACTAGAATGG*GAGACCGCGGTCCCGAATTC*
***GAGCTCGGTACCCGGGGATCCCTCGAGGTCGACCTGCAGGGGGACCATGGTCTC*TG**
ATAAGccaggcatcaaataaaacgaaaggctcagtcgaaagactgggcctttcgttttatctgttgtttgtcggtgaacgctctc

Figure 9. Agarose gels confirming positive Lux constructs. (a) BamHI/HindIII digest with positive bands at ~2938bp and 2634bp for p264pLux and positive bands at ~4203bp and 3100bp for p264pLux-uidA; (b) BamHI/HindIII digest with positive bands at ~2938bp and 2634bp for p452pLux and a positive band at ~6200bp for p452LuxR; (c) BamHI/HindIII digest with positive bands at ~3100bp and 4224bp for p452pLux-uidA; (d) BamHI/HindIII digest with positive bands at ~3100bp and 3912bp for p0169pLux-uidA; (e) pLux sequence, bold letters indicate Lux promoter region, italicized letters indicate MCS region, and lowercase indicates terminator region. Panels a-d are a composite of multiple agarose gels adjusted to the observed sizes.

Construction of ATc Inducible Promoter Systems. Three ATc inducible systems were created by cloning the *tetR* gene into pBBR1p264-pelB-STL and pBBR1p452-STL to create p264-TetR and p452TetR (Figure 10 and 11). The promoter p452 was then replaced with p0169 (Shi et al., 2014) in the p452TetR plasmid to create p0169TetR. A synthesized DNA fragment containing the Tet promoter, RBS, MCS, and terminator (Florea et al., 2016) (Figure 11) was cloned into p264-TetR, p452TetR, and p0169TetR plasmids to create p264pTet, p452pTet, and p0169pTet (Figure 10 and 11).

Proofs of concept constructs were created by cloning *uidA* into the MCS of p264pTet, p452pTet, and p0169pTet to create p264pTet-uidA, p452pTet-uidA, and p0169pTet-uidA (Figure 10 and 11). The p264pTet, p452pTet, p0169pTet p264pTet-uidA, p452pTet-uidA, and p0169pTet-uidA were all transformed by electroporation into *G. oxydans*.

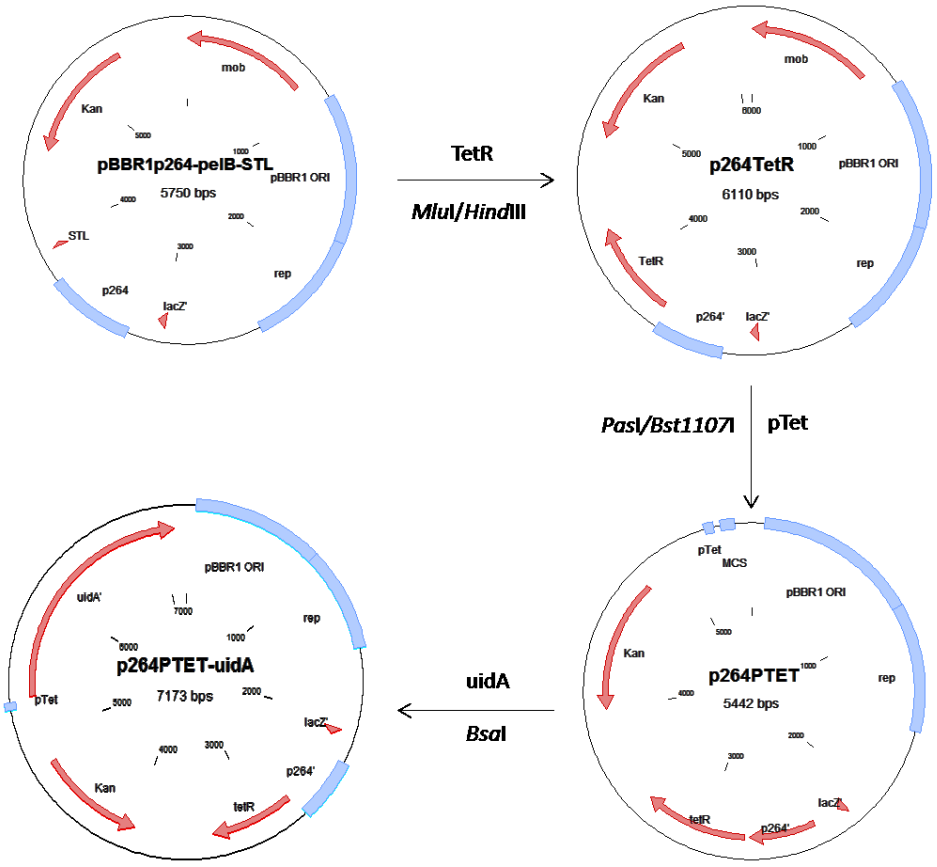

Figure 10. Construction of the Tet system. Vector maps of pBBR1p264-*pelB*-STL, p264TetR, p264pTet, and p264pTet-uidA. Plasmid p264TetR was created by ligating TetR amplicon cut with HindIII and MluI into similarly cut pBBR1p264-*pelB*-STL. Plasmid p2654pTet was created by ligating the pTet DNA fragment cut with PasI and Bst1107I with similarly cut p264TetR. Plasmid p264pTet-uidA was created by ligating the *uidA* amplicon cut with BsaI into similarly cut p264pTet. Construction of p452pTet-uidA and p0169pTet-uidA were done similarly.

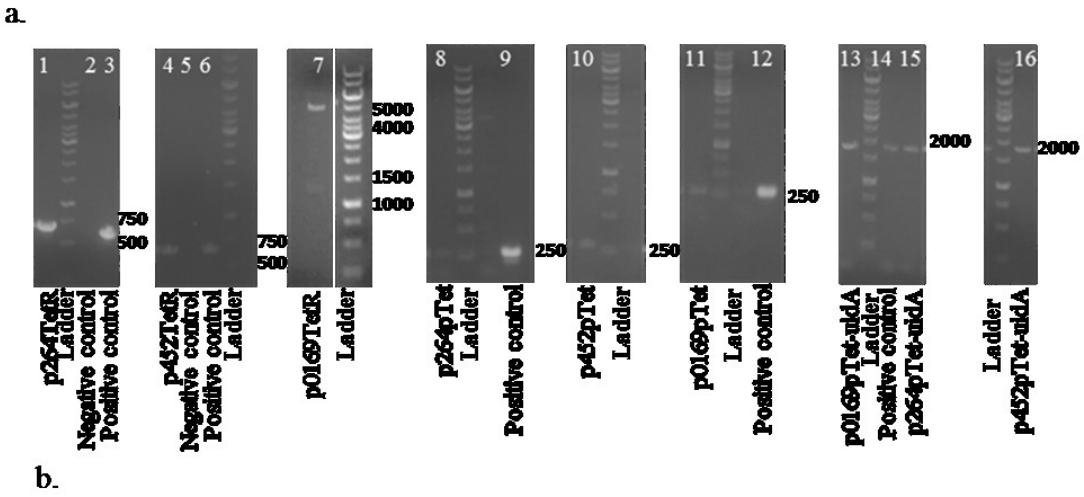

Figure 11. Agarose gels confirming positive Tet constructs. (a) Lane 1 positive band at ~660bp, lane 2 negative control with no band, lane 3 positive control band at ~660bp, lane 4 positive band at ~660bp, lane 5 negative control with no band, lane 6 positive control band at ~660bp, lane 7 restriction digest of p0169 with positive bands at ~4596bp and 1223bp, lane 10 positive colony PCR bands at ~270bp, lane 11 positive colony PCR bands at ~270bp, lane 12 positive control band at ~270bp, lane 13 *uidA* positive colony PCR bands at ~1800bp, lane 14 positive control band at ~1800bp, lane 15 *uidA* positive colony PCR bands at ~1800bp, lane 16 *uidA* positive colony PCR bands at ~1800bp. The figure is a composite of multiple agarose gels adjusted to the observed sizes. (b) pTet sequence shown below gel images, bold letters indicate Tet promoter region, italicized letters indicate MCS region, and lowercase indicates terminator region.

Lux UidA Assays. To assess if the Lux system could be used to control gene expression in *G. oxydans*, cells containing the p264pLux, p452pLux, p0169pLux, p264pLux-uidA, p452pLux-uidA, and p0169pLux-uidA were assayed for inducible UidA activity as described above (see section 2.11). The empty vector negative controls (p264pLux, p452pLux, and p0169pLux) did not produce a yellow color in the presence of PNPG. This was expected as these constructs lacked a UidA enzyme. The uninduced controls containing the UidA enzyme did produce a low basal level of β-glucuronidase

(UidA) activity. However, when induced, UidA activity increased dramatically. The p0169pLux-uidA constructs induced with 0, 1, 5, and 10μM of AHL had average UidA activities of 1077.0, 5916.7, 5508.0, and 5558.7 Miller Units, respectively (Figure 12), which is about 5.25 ± 0.21 times higher than uninduced levels ($q<0.0001$, Table 3). The induced p264pLux-uidA constructs had activities 3.42 ± 0.17 times higher than uninduced ($q<0.0001$, Table 4), corresponding to average activities of 1303.9, 4690.0, 4249.0, and 4436.7 Miller Units when induced with 0, 1, 5, and 10μM of AHL, respectively (Figure 13). Whereas the p452pLux-uidA constructs induced with 0, 1, 5, and 10μM of AHL had average UidA activities of 2277.2, 10563.4, 9421.3, and 9610.9 Miller Units (Figure 14), which is approximately 4.33 ± 0.27 times higher than uninduced levels ($q<0.0001$, Table 5). Interestingly, in all cases the average UidA activities were similar regardless of the amount of AHL used to induce gene expression (Figure 12-14).

Tet UidA Assays. *G. oxydans* cells containing the p264pTet, p452pTet, p0169pTet, p264pTet-uidA, p452pTet-uidA, and p0169pTet-uidA plasmids were assayed as described for the Lux system except 0, 100, 200 or 500 ng/mL of ATc was used for induction. The empty vector negative controls lacking UidA (p264pTet, p452pTet, and p0169pTet) did not produce a yellow color in the presence of PNPG. Cells that contained the UidA enzyme all had some UidA activity whether or not they were induced with ATc. In cells containing p264pTet-uidA and p452pTet-uidA, activity in induced cells was similar to that of uninduced cells (Figure 15). There was an average of 1.83 ± 0.13 times higher activity in ATc induced cells containing p264pTet-uidA, having average UidA activities of 195.0, 352.8, 335.0 and 383.9 Miller Units when induced with 0, 100, 200, and 500μM of ATc, respectively. Cells containing p452pTet-uida had average UidA

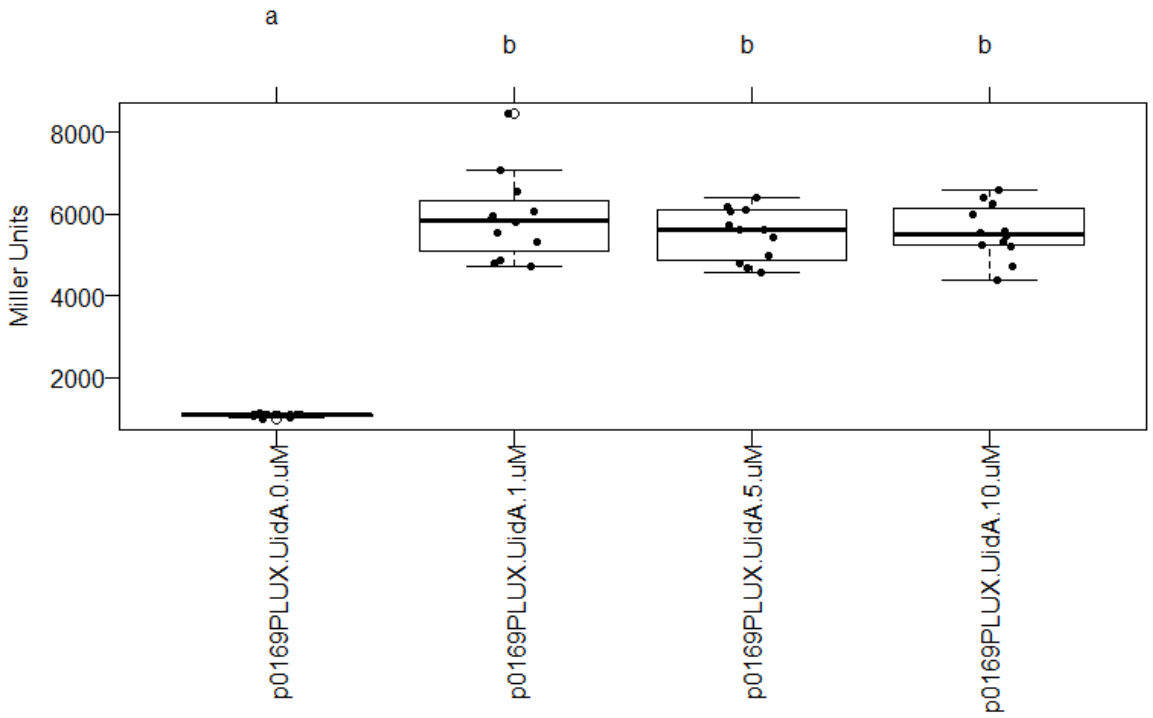

Figure 12. AHL induced UidA activity in cells containing p0169pLux-uidA**.** Letters above the plot denote statistical groups and were determined by an ANOVA and *post-hoc* Tukey's HSD test.

Table 3: Statistical analysis for p0169pLux-uidA induction

	0µM	1µM	5µM	10µM
0µM	-	<0.0001	<0.0001	<0.0001
1µM	-	-	0.490	0.599
5µM	-	-	-	0.998

q values from an ANOVA and *post-hoc* Tukey's HSD test

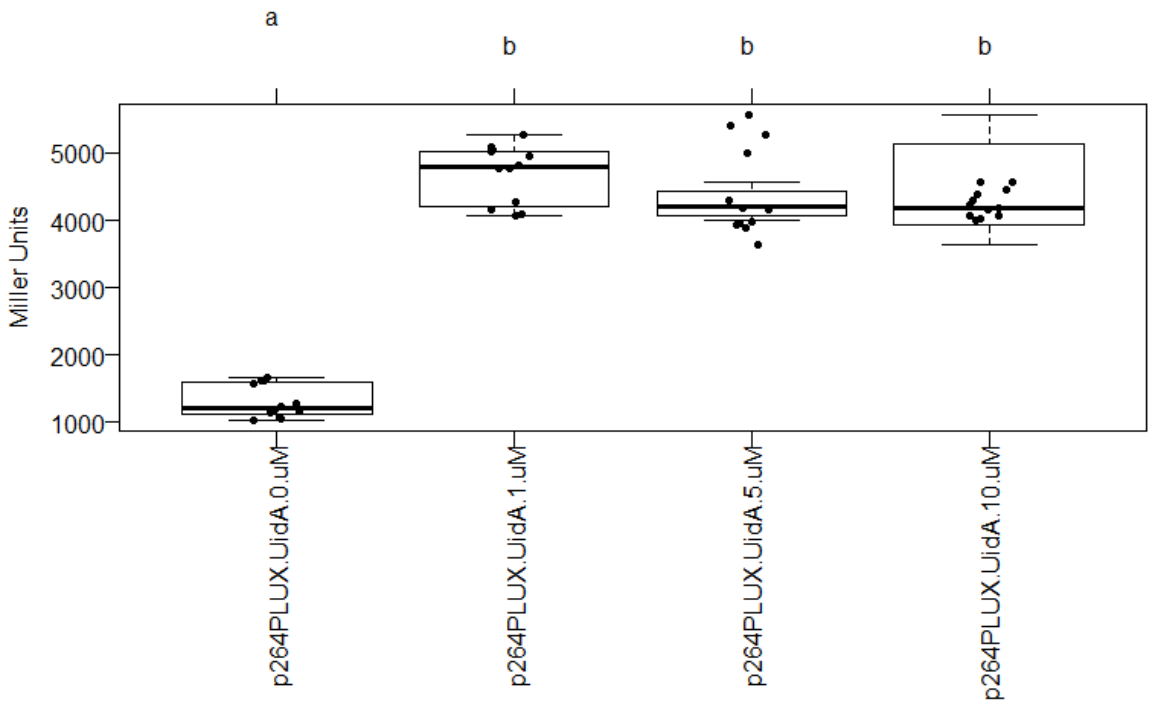

Figure 13. AHL induced UidA activity in cells containing p264pLux-uidA. Letters above the plot denote statistical groups and were determined by an ANOVA and *post-hoc* Tukey's HSD test.

Table 4: Statistical analysis for p264pLux-uidA induction

	0µM	1µM	5µM	10µM
0µM	-	<0.001	<0.001	<0.001
1µM	-	-	0.073	0.483
5µM	-	-	-	0.712

q values from an ANOVA and *post-hoc* Tukey's HSD test

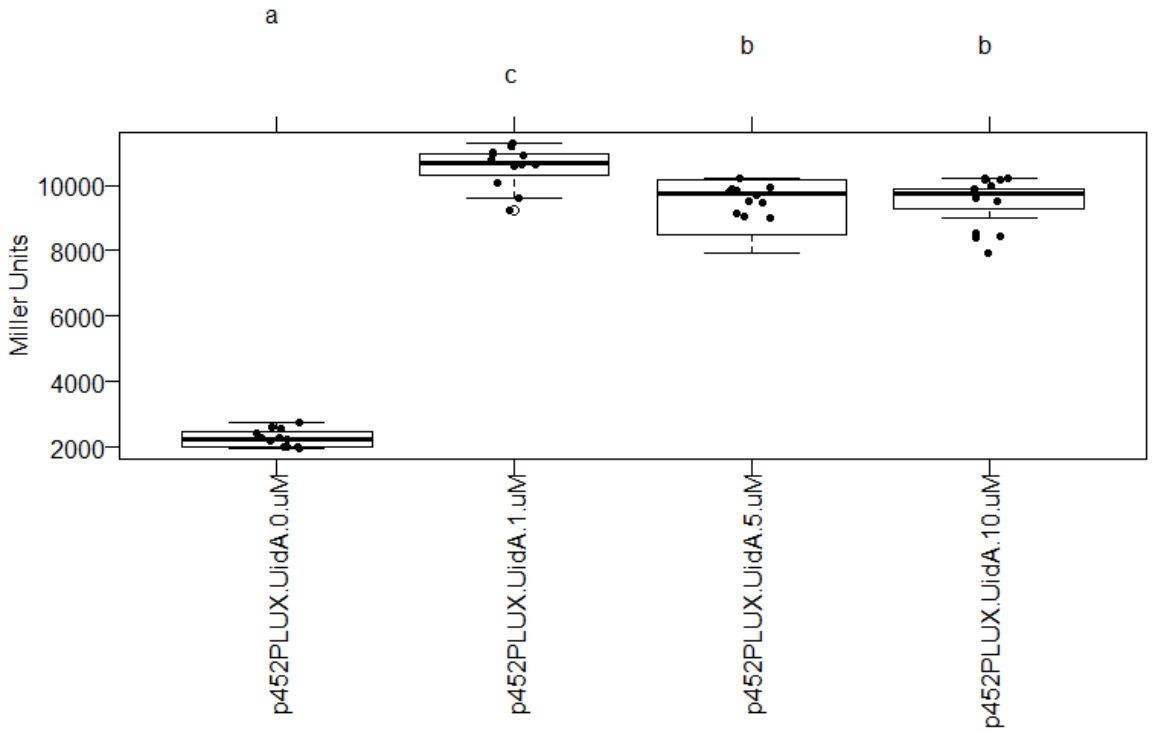

Figure 14. AHL induced UidA activity in cells containing p452pLux-uidA. Letters above the plot denote statistical groups and were determined by an ANOVA and *post-hoc* Tukey's HSD test.

Table 5: Statistical analysis for p452pLux-uidA induction

	0μM	1μM	5μM	10μM
0μM	-	<0.0001	<0.0001	<0.0001
1μM	-	-	<0.0001	0.00118
5μM	-	-	-	0.85277

q values from an ANOVA and *post-hoc* Tukey's HSD test

activities of 790.0, 566.9, and 551.0 Miller Units when induced with 100, 200, and 500 μM of ATc. These activities correspond to approximately 2.16 ± 0.45 times higher activity compared to uninduced levels (294.3 Miller Units). *G. oxydans* containing p0169pTet-uida had an average of 6.23 ± 1.21 times higher UidA activity when induced,

regardless of the concentration of ATc. Average UidA activities were 652.0, 4574.0, 4453.2, and 3159.3 Miller Units when induced with 0, 100, 200, and 500µM of ATc, respectively. However, activities were highly variable and clustered tightly according to biological replicates, creating two distinct groups for each concentration of ATc. UidA activities ranged from 2478 Miller Units to 6805 Miller Units in cells induced with 100ng/mL ATc, from 2634 Miller Units to 6568 Miller Units in cells induced with 200ng/mL ATc, and from 1821 Miller Units to 4678 Miller Units in cells induced with 500ng/mL ATc. This pattern was also observed, although not as dramatically, in *G. oxydans* containing p264pTet-uida or p452pTet-uida (Figure 15).

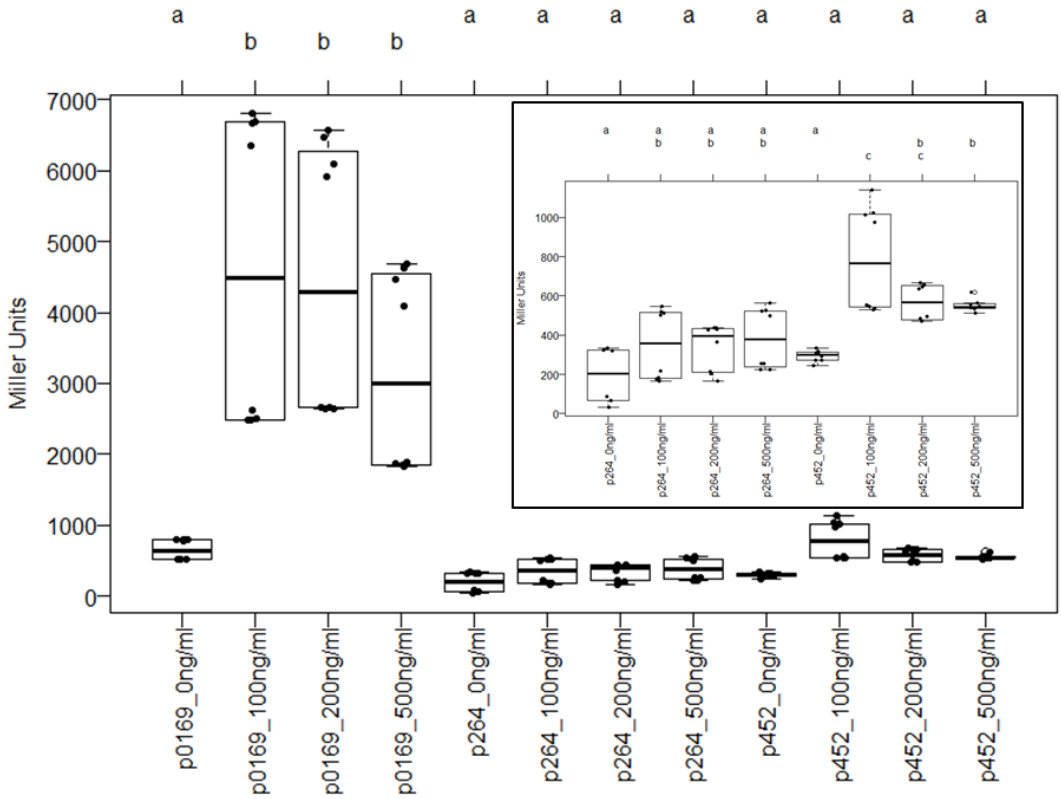

Figure 15. ATc induced UidA activity in *G. oxydans* Data for the first five minutes after PNPG addition were analyzed. Letters above the plot denote statistical groups and were determined by an ANOVA and *post-hoc* Tukey's HSD test.

DISCUSSION

Fluorescent Protein-based Reporter Systems

Two fluorescent protein based reporter systems were designed to facilitate rapid screening of positive clones in *G. oxydans*. Because the empty vectors pBBR1p(264/452)-Xa-(GFPuv/mRFP)-STL were constructed without adding a ribosomal binding site to the 5' end of the Xa-FP fusions, only cells containing plasmids with the protein of interest with a RBS inserted upstream of the fluorescent reporter system were expected to produce fluorescence. However, even *G. oxydans* that contained empty vectors fluoresced. The same was true for *E. coli* cells harboring the empty vectors (Figure 16). Such systems have been utilized successfully in *E. coli* including one constructed for overexpression and purification of membrane proteins using a TEV protease recognition site, GFP reporter, and an 8His purification tag (Drew et al., 2006). This indicates that there may be a cryptic RBS either upstream of the Xa-FP fusion or within the sequence encoding the Xa recognition site.

A previous attempt to create a fluorescent-based reported system for G. oxydans involved using a Xa-Pp1 fusion as a fluorescent reporter (Pearson, 2014). This construct also gave background fluorescence with the empty vector controls. It was hypothesized that the Xa protease sequence (5'-ATCGAGGGAAGG-3') could be acting as a RBS, allowing for the translation of Pp1 (Pearson, 2014). In this study, the Xa protease sequence was optimized (5'-ATCGATGGTCGC-3') to reduce the possibility of ribosomal binding. The original Xa protease described by Pearson, 2014 has a predicted RBS translational rate of 496 AU, which is 1.8-fold higher than the predicted rate (276.5

AU) for the optimized Xa protease sequence used here (Borujeni et al., 2013; Salis et al., 2009, https://salislab.net/software). It is conceivable that the optimized Xa protease sequence is still able to direct translation even with this reduced activity, resulting in the leaky expression in vectors only containing the Xa protease recognition site (Figure 6 and 7). It is important to note that the native RBS of gox2015 intended to direct translation has a predicted RBS translation rate of 331 AU, which is only slightly greater than the optimized Xa protease sequence. One way to determine whether Xa recognition sequence could be acting as a weak RBS would be to create a construct where a GS linker replaces the Xa protease recognition sequence altogether. If the empty vector cells do not fluoresce, then creating a new construct using a different protease recognition site might mitigate the background fluorescence from the empty vector clones.

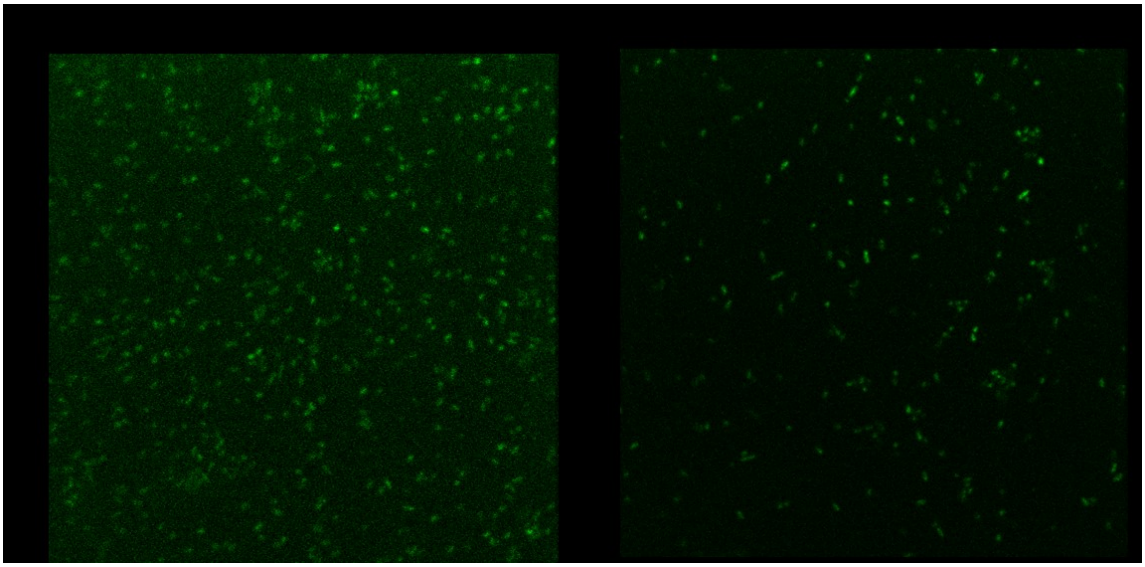

Figure 16. *E. coli* cells expressing GFPuv. (a) *E. coli* 10β cells harboring the pBBR1p452-Xa-GFPuv-STL plasmid; (b) *E. coli* cells harboring the pBBR1p452-*gox2015*-Xa-GFPuv-STL plasmid.

Inducible Promoter Systems

Two inducible systems were constructed and assayed for their ability to regulate gene expression in *G. oxydans*. The Lux system induced by AHL was highly regulatable with up to 5.25 times higher UidA activity than the uninduced level. Similarly, the Tet system induced by ATc was also regulatable with up to 7 times higher UidA activity than the uninduced level. However, induction by ATc was also highly variable. When several similar AHL and ATc inducible systems were investigated to regulate cellulose production in *Komagataeibacter rhaeticus,* another member of the *Acetobacteraceae* family, the Lux systems had higher induction and lower basal expression of mRFP than the Tet systems (Florea et al., 2016). The lack of tight regulation and unreliability of the ATc inducible system suggests it is not an optimal candidate for regulatable gene expression in *G. oxydans*. Conversely, the Lux system provides predictable induction levels and is tightly controlled, making it a suitable regulatable promoter in *G. oxydans* and other acetic acid bacteria.

In addition to the constitutive promoters, p264 and p452, a third *G. oxydans* promoter, p0169, was investigated. Strengths of these three promoters, as well as that of *tufB*, were assessed previously by comparing the fluorescence intensity of GFP expressed under the control of each promoter (Yuan et al, 2016). Of the four promoters, p0169 was found to be the strongest, followed closely by p264, p452, and *tufB*. Placing the expression of LuxR or TetR under the control of a stronger promotor was expected to increase regulatory control. Of the Lux constructs, those with the strongest constitutive promoters, p0169 and p264, controlling transcription of the *luxR* transcriptional activator gene were expected to produce the highest level of UidA induction. While the highest

induction compared to the basal level was observed with the construct with the strongest promoter, p0169, the weakest of the three promoters, p452, produced the highest total activities after induction (Figure 17). However, the p452 promoter also produced approximately double the basal level of enzyme activity when uninduced. It is possible that when UidA is highly overproduced it forms inclusion bodies, making much of its activity undetectable. Alternatively, overproduction of LuxR could have formed inclusion bodies, making much of the protein unavailable to activate the Lux promoter. In fact, LuxR is known to form inclusion bodies when overexpressed in *E. coli* (Kaplan and Greenberg, 1987). This could also explain why there was only near basal level induction of the Tet promoter when induced by ATc with both the p264 and p452 promoters. If the p0169 overproduces TetR to the point that inclusion bodies are formed, less of the protein would be available to bind to and repress the Tet promotor. In this case, lower levels of TetR production would mitigate inclusion body formation, making more of the repressor available to bind to the Tet promotor. The formation of inclusion bodies may also lead to abnormal cell division. This phenomenon has been previously observed in *E. coli* (Lee et al., 2008). Indeed, when *G. oxydans* cells harboring the p0169pLux, p264pLux, p452pLux, p0169pTet, p264pTet, and p452pTet plasmids were observed by brightfield microcopy, they were frequently elongated compared to wildtype cells (Figure 18). Additionally, *G. oxydans* cells harboring the fluorescent reporter constructs pBBR1p264-*gox2015*-Xa-RBS-mRFP-STL or pBBR1p452-*gox2015*-Xa-GFPuv-STL were also frequently elongated (Figure 6 and 7). Similar abnormalities in morphology have been reported *G. oxydans* cells harboring fluorescent reporter constructs (Pearson, 2014). This

could indicate that *G. oxydans* also forms inclusion bodies and fails to divide properly when proteins are overproduced in the cell.

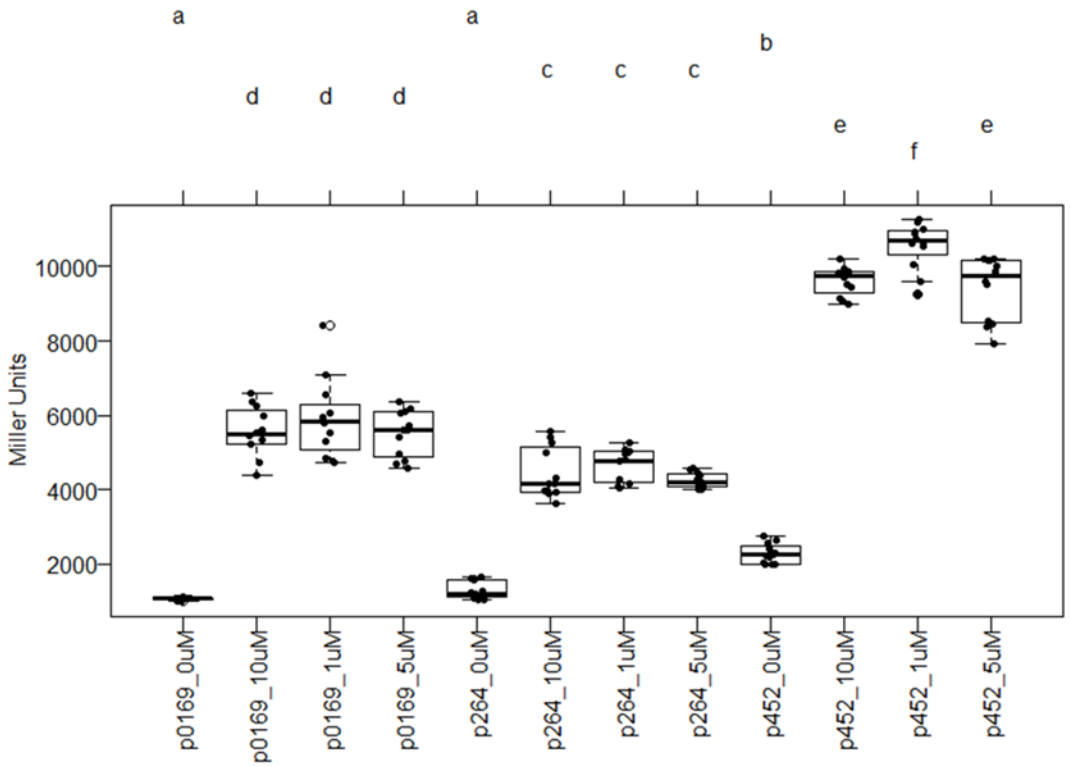

Figure 17. Lux promoter-mediated β-Glucuronidase activity in AHL induced cells**.** The highest activity was seen in cells containing the p452pLux-uidA plasmids. Data included in analyses are from 4 technical replicates of each of 3 biological replicates (n=12).

The Lux system showed promise as a candidate for gene regulation in *G. oxydans*, but it may be beneficial to further reduce basal level expression in the uninduced state. In *A. fischerii*, the AHL is produced by a synthase encoded by the *luxI* gene. The expression of the *luxI* gene, along with the other bioluminescence genes is under the control of the activator, LuxR. (Fuqua et al., 1994). Yet, basal levels of AHL are still produced. It may

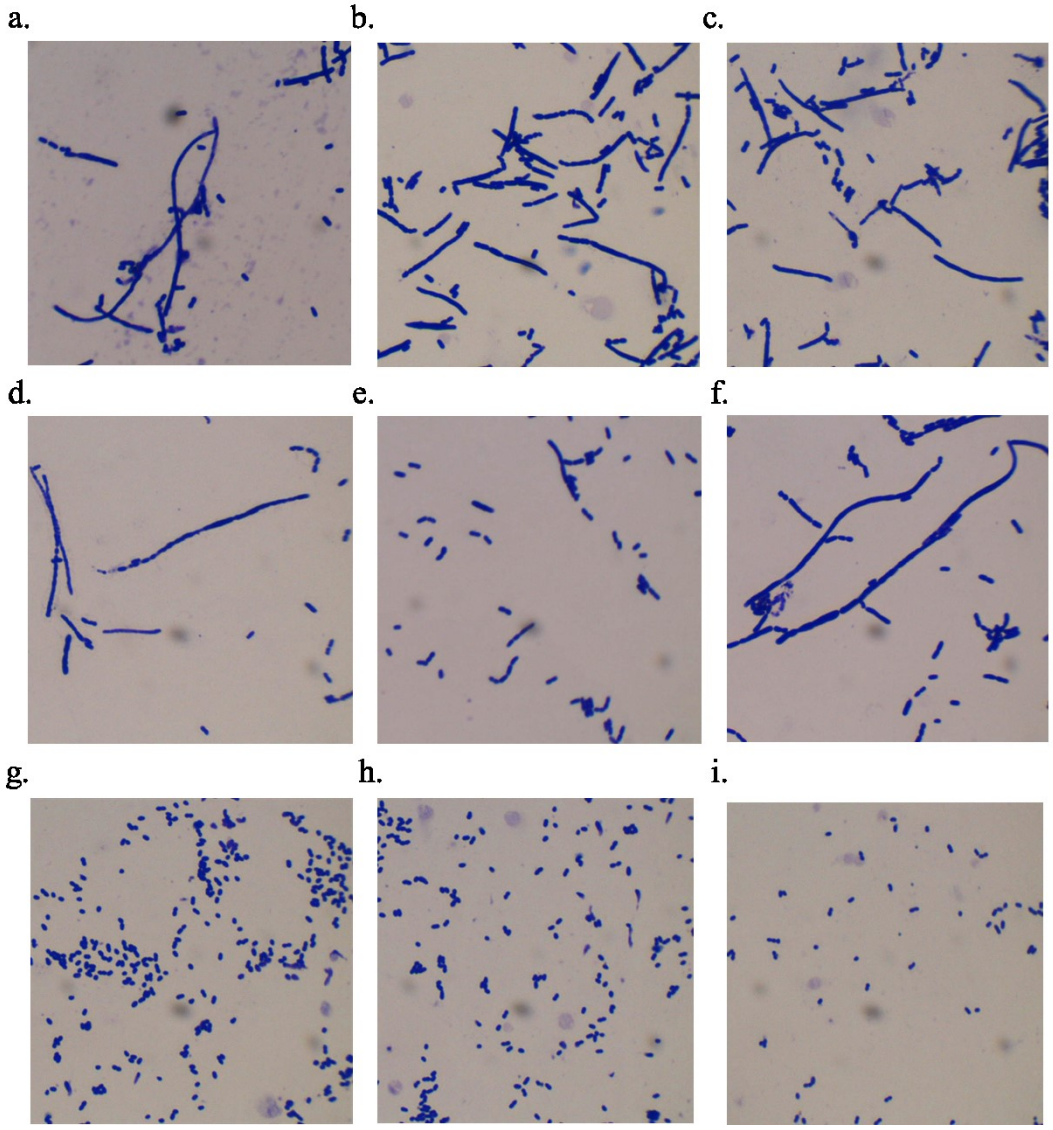

Figure 18. Brightfield microscopy of *G. oxydans* cells stained with crystal violet. (a) *G. oxydans* cells harboring the p0169pLux plasmid; (b) *G. oxydans* cells harboring the p264pLux plasmid; (c) *G. oxydans* cells harboring the p452pLux plasmid; (d) *G. oxydans* cells harboring the p0169pTet plasmid; (e) *G. oxydans* cells harboring the p264pTet plasmid; (f) *G. oxydans* cells harboring the p452pTet plasmid; (g-i) Wildtype cells displaying typical cell morphology. Representative images are shown.

be that LuxR has weak binding affinity for the Lux promoter without interacting with the AHL, providing leaky transcription in *G. oxydans*. Placing the *luxR* gene under the

control of a regulatable promoter could provide better control over transcription of the target gene. However, if the holo-RNA polymerase binds the *lacI* promoter weakly in the absence of LuxR to provide constitutive background levels of LuxI or if *G. oxydans* produces its own AHL or an AHL-like metabolite, more fine-tuned control may not be possible using this system. To date, quorum sensing has not been documented in *G. oxydans*, but in a related species, *Gluconacetobacter intermedius*, quorum sensing via a GinI/GinR system has been reported (Iida et al., 2008). In the GinI/GinR system, GinI synthesizes three AHLs and GinR is a transcriptional regulator. There are no known homologs to GinR or GinI found in *G. oxydans* based on BLASTp, making it unlikely that this system exists in *G. oxydans*. However, there is little known about the regulatory mechanisms of *G. oxydans*, and it is possible other undiscovered Lux-like systems exist in this bacterium that may be at least partially compatible with the LuxR/LuxI system. The lack of knowledge about gene regulation in *G. oxydans* highlights the need for better molecular tools to facilitate more research into its regulatory mechanisms.

REFERENCES

Bertrand, K. P., Postle, K., Wray, L. V., & Reznikoff, W. S. (1983). Overlapping divergent promoters control expression of Tn10 tetracycline resistance. *Gene, 23*(2), 149-156.

Borujeni, A. E., Channarasappa, A. S., & Salis, H. M. (2013). Translation rate is controlled by coupled trade-offs between site accessibility, selective RNA unfolding and sliding at upstream standby sites. *Nucleic Acids Res*, *42*(4), 2646-2659.

Chung, C. T., Niemela, S. L., & Miller, R. H. (1989). One-step preparation of competent *Escherichia coli*: transformation and storage of bacterial cells in the same solution. *Proc Natl Acad Sci U S A, 86*(7), 2172-2175.

Drew, D., Lerch, M., Kunji, E., Slotboom, D. J., & de Gier, J. W. (2006). Optimization of membrane protein overexpression and purification using GFP fusions. *Nat Methods, 3*(4), 303-313.

Deppenmeier, U., Hoffmeister, M., & Prust, C. (2002). Biochemistry and biotechnological applications of *Gluconobacter strains*. *Appl Microbiol Biotechnol, 60*(3), 233-242.

Florea, M., Hagemann, H., Santosa, G., Abbott, J., Micklem, C. N., Spencer-Milnes, X., de Arroyo Garcia, L., Paschoua, D., Lazenbatta, C., Kong, D., Chughtai, H., Jensen, K., Freemont, P. S., Kitney, R., Reeve B., & Ellis T. (2016). Engineering control of bacterial cellulose production using a genetic toolkit and a new cellulose-producing strain. *Proc Natl Acad Sci U S A, 113*(24), E3431-E3440.

Fuqua, W. C., Winans, S. C., & Greenberg, E. P. (1994). Quorum sensing in bacteria: the LuxR-LuxI family of cell density-responsive transcriptional regulators. *J Bacteriol, 176*(2), 269.

Gosselé, F., Swings, J., Kersters, K., & De Ley, J. (1983). Numerical analysis of phenotypic features and protein gel electropherograms of *Gluconobacter Asai* 1935 emend. mut. char. Asai, Iizuka, and Komagata 1964. *Int J Syst Evol Microbiol, 33*(1), 65-81.

Gupta, A., Singh, V. K., Qazi, G. N., & Kumar, A. (2001). *Gluconobacter oxydans*: its biotechnological applications. *J Mol Microbiol Biotechnol, 3*(3), 445-456.

Iida, A., Ohnishi, Y., & Horinouchi, S. (2008). An OmpA family protein, a target of the GinI/GinR quorum-sensing system in *Gluconacetobacter intermedius*, controls acetic acid fermentation. *J Bacteriol, 190*(14), 5009-5019.

Kallnik, V., Meyer, M., Deppenmeier, U., & Schweiger, P. (2010). Construction of expression vectors for protein production in *Gluconobacter oxydans*. *J Biotechnol, 150*(4), 460-465.

Kaplan, H. B., & Greenberg, E. P. (1987). Overproduction and purification of the *luxR* gene product: Transcriptional activator of the *Vibrio fischeri* luminescence system. *Proc Natl Acad Sci U S A, 84*(19), 6639–6643.

Kosciow, K., Domin, C., Schweiger, P., & Deppenmeier, U. (2016). Extracellular targeting of an active endoxylanase by a TolB negative mutant of *Gluconobacter oxydans*. *J Ind Microbiol Biotechnol, 43*(7), 989-999.

Kosciow, K., Zahid, N., Schweiger, P., & Deppenmeier, U. (2014). Production of a periplasmic trehalase in *Gluconobacter oxydans* and growth on trehalose. *J Biotechnol, 189*, 27-35.

Kostner, D., Peters, B., Mientus, M., Liebl, W., & Ehrenreich, A. (2013). Importance of *codB* for new *codA*-based markerless gene deletion in *Gluconobacter* strains. *Appl Microbiol Biotechnol, 97*(18), 8341-8349.

Lee, K. K., Jang, C. S., Yoon, J. Y., Kim, S. Y., Kim, T. H., Ryu, K. H., & Kim, W. (2008). Abnormal cell division caused by inclusion bodies in *E. coli*; increased resistance against external stress. *Microbiol Res, 163*(4), 394-402.

Levering, P. R., Weenk, G., Olijve, W., Dijkhuizen, L., & Harder, W. (1988). Regulation of gluconate and ketogluconate production in *Gluconobacter oxydans* ATCC 621-H. *Arch Microbiol, 149*(6), 534-539.

Matsushita, K., Fujii, Y., Ano, Y., Toyama, H., Shinjoh, M., Tomiyama, N., Miyazaki, T., Sugisawa, T., Hoshino, T., & Adachi, O. (2003). 5-Keto-D-gluconate production is catalyzed by a quinoprotein glycerol dehydrogenase, major polyol dehydrogenase, in *Gluconobacter* species. *Appl Environ Microbiol, 69*(4), 1959-1966.

Miller, J.H. (1972). Unit VII: Assays of lac operon enzymes: beta-galactosidase, permease, repressor, transacetylase, a complementation. In Miller, J.H. (Ed.), *Experiments in Molecular Genetics* (pp. 352–355). Cold Spring Harbor, NY. Cold Spring Harbor Laboratory Press.

Pearson, K.P. (2014). The Development of genetic tools to aid in protein characterization for use in the acetic acid bacterium *Gluconobacter oxydans* (Master's thesis). Missouri State University, Springfield, MO.

Peters, B., Junker, A., Brauer, K., Mühlthaler, B., Kostner, D., Mientus, M., Liebl, W., & Ehrenreich, A. (2013a). Deletion of pyruvate decarboxylase by a new method for efficient markerless gene deletions in *Gluconobacter oxydans*. *Appl Microbiol Biotechnol, 97*(6), 2521-2530.

Peters, B., Mientus, M., Kostner, D., Junker, A., Liebl, W., & Ehrenreich, A. (2013b). Characterization of membrane-bound dehydrogenases from *Gluconobacter oxydans* 621H via whole-cell activity assays using multideletion strains. *Appl Microbiol Biotechnol, 97*(14), 6397-6412.

Prust, C., Hoffmeister, M., Liesegang, H., Wiezer, A., Fricke, W. F., Ehrenreich, A., Gottshalk, G., & Deppenmeier, U. (2005). Complete genome sequence of the acetic acid bacterium *Gluconobacter oxydans*. *Nat Biotechnol, 23*(2), 195-200.

R Core Team (2013). R: A language and environment for statistical computing. R Foundation for Statistical Computing, Vienna, Austria. URL http://www.R-project.org/

Salis, H. M., Mirsky, E. A., & Voigt, C. A. (2009). Automated design of synthetic ribosome binding sites to control protein expression. *Nat Biotechnol*, *27*(10), 946-950.

Shi, L., Li, K., Zhang, H., Liu, X., Lin, J., & Wei, D. (2014). Identification of a novel promoter gHp0169 for gene expression in *Gluconobacter oxydans*. *J Biotechnol, 175*, 69-74.

Skerra, A. (1994). Use of the tetracycline promoter for the tightly regulated production of a murine antibody fragment in *Escherichia coli*. *Gene*, 151(1), 131-135.

Yuan, J., Wu, M., Lin, J., & Yang, L. (2016). Combinatorial metabolic engineering of industrial *Gluconobacter oxydans* DSM2343 for boosting 5-keto-D-gluconic acid accumulation. *BMC Biotechnol, 16*(1), 42.